Journal of Advanced Joining Processes 5 (2022) 100110

Contents lists available at ScienceDirect

Journal of Advanced Joining Processes

journal homepage: www.sciencedirect.com/journal/journal-of-advanced-joining-processes

A review of LTT welding alloys for structural steels: Design, application and results

Victor Igwemezie [a,c,*], Muhammad Shamir [b], Ali Mehmanparast [b], Supriyo Ganguly [a]

[a] Welding Engineering and Laser Processing Centre, Cranfield University, UK
[b] Dept. of Naval Architecture, Ocean and Marine Engineering, University of Strathclyde, UK
[c] Dept. of Materials & Metallurgical Engineering, Federal University of Technology, Owerri, Nigeria

ARTICLE INFO

Keywords:
Steel
Welding
Residual stress
Fatigue strength
LTT alloy
Microstructure
Austenite
Martensite

ABSTRACT

A great deal of effort goes into production of modern steel for structural applications. The structural integrity of the steel becomes compromised when it is welded to form engineering components. The structural capacity of the steel joints is further reduced if the joint is to serve in a fluctuating stress environment. This is because, the fatigue strength (FS) of the steel structure is now shifted to the welded joints. One of the major factors that deteriorate the FS of welded joints is tensile residual stress (TRS). There have been efforts in the last two decades to develop welding alloys capable of mitigating TRS in welded joints based on the phase-transformation of austenite (γ) to martensite (ά). This paper reviews the design, application and results of these alloys often referred to as Low Transformation Temperature (LTT) welding alloys. It also presented the factors affecting them and areas where performance data are lacking.

Introduction

The welding process is indispensable in the joining of structural members in most engineering structures. However, welding as a localised heating strategy strongly influences the structural performance of the welded component. The structural capacity of the steel is significantly reduced when it is welded to form components. It becomes a safety critical issue when a welded steel component is to serve in a fatigue environment. This is because, the fatigue strength (FS) of the steel now lies on the welded joints. For example, the FS of unwelded steel specimen generally increases with increase in the material's yield strength (YS) (Watanabe et al., 1995) (Ota et al., 2000). But the yield strength (YS) of the base metal has no effect on the FS of the welded structure irrespective of the joint type. It has been reported that ~ 80% of mechanical failures are fatigue related (Nose and Okawa, 2012). FS is commonly measured by the highest stress the weld joint can withstand for a given number of cycles without failure. One of the major factors that deteriorate the FS of welded joints is residual stress (RS) (K. Masubuchi, 1980) (Fricke, 2005) (Ainsworth et al., 2000) (JA Francis et al., 2007). This phenomenon tends to arise due to differential thermal expansion and contraction following solidification of the molten weld metal (WM) (PJ Withers and Bhadeshia, 2001) (PJ Withers and Bhadeshia, 2001). Fig. 1 shows two types of RS that are commonly identified in welded joints – the tensile residual stress (TRS) and compressive residual stress (CRS). One type arises to equilibrate the other force. The magnitude and orientation of the RS can be affected by the heat source (Plasma, laser or arc), degree of mechanical constraints (rigid or lax), weld joint geometry ((butt, fillet, gusset, box), temperature-dependant material properties (thermal expansion and conductivity), thermal history (quenched or free cooling) and weld metal (WM) phase transformation (e.g. austenite (γ) to martensite (ά)) (Coules, 2013) (Leggatt, 2008) (Colegrove et al., 2009). The RS orientations and magnitudes in the longitudinal (L) and transverse (T) are commonly depicted as shown in Fig. 1. From the directions of the RS, if a crack is present at the weld toe, the transverse TRS will matter most since it is acting to open and propagate the crack in mode I fatigue (Zerbst, 2020). The transverse TRS combines with the applied service stress to increase the magnitude of the mean stress. The increased crack driving force increases the propagation rate of defects to failure.

The combined effects of defects and RS contribute significantly to the limit of load that can be imposed on the structural member (K. Masubuchi, 1980). Thus, TRS is a strong limiting factor in the structural integrity of welded joints. While the TRS is damaging to fatigue life, the CRS is found to enhance it. To supress the contributions of the TRS around vulnerable areas of the welded joints, post weld treatment is often carried out to relieve the RS (Cheng et al., 2003). Peening operation is used to induce compressive stress on the surface area of interest to

* Corresponding author.
E-mail address: victor.igwemezie@cranfield.ac.uk (V. Igwemezie).

https://doi.org/10.1016/j.jajp.2022.100110

Available online 6 April 2022

Key nomenclature

CRS	compressive residual stress
FCG	fatigue crack growth
FCGR	fatigue crack growth rate
FS	fatigue strength
$Ms._T$	martensite start temperature
LTT	low transformation temperature
LWM	LTT weld metal
LTTW	LTT wire
WM	weld metal
RS	residual stress
T_a	ambient temperature
T_i	interpass temperature
TRS	tensile residual stress
TS	tensile strength
YS	yield strength
α_b	bainite
α	ferrite
δ	delta ferrite
ά	martensite
γ	austenite
γ_r	retained austenite

retard crack initiation and premature failure (Habibi et al., 2012) (Abdullah et al., 2012) (Kou, 2003). Unfortunately, the post weld treatment and peening can add substantially to the cost of fabrication. To eliminate this cost, it was proposed (Jones and Alberry, 1977) that strains associated with the solid-state transformation of martensite (ά) could be exploited to design welding alloys that could mitigate the TRS. In this way, no post weld heat treatment would be needed. The simple reasoning is that the (γ) is face centred-cubic (*fcc*) while the ά has body centred-tetragonal (*bct*) structure (Bhadeshia, 2004). The volume of *bct* unit cell is larger than *fcc*. When ά transforms from γ, there will be a volume increase (Bhadeshia and Honeycombe, 2006) (Bhadeshia et al., 2007) (HKDH. Bhadeshia, 2002). In a constrained state, the volume increase will induce CRS in the area around the transformed WM. This phenomenon has been exploited to design Low Transformation Temperature (LTT) welding alloys that can induce CRS at areas prone to stress concentration such as the weld toe.

Fig. 2 illustrates the kind of forces that could be induced along the weld length when conventional and the so-called LTT wire (LTTW) are used. For the conventional wire (Fig. 2(a)), shrinkage dominates, compressive stress builds up at the plate edges and TRS builds up towards the mid plate of the weld centreline. In the case of LTT wire (LTTW) (Fig. 2(b)), the reverse should be the case if we imagined that a cut is made along the centreline of the weld as shown.

Fig. 2 (c & d) are often used to illustrate the concept of mitigation of the thermal strain by phase transformation. Fig. 2(c) is a T-joint fillet welded with a conventional weld wire. Shrinkage of the WM resulted to distortion as shown. In Fig. 2(d), the distortion caused by using conventional weld wire is relaxed by using the filler capable of transforming to ά at low temperatures. In the LTT weld, the expansion caused by the WM resulted to reduction in the welding distortion (Thomas and Liu, 2014). This finding is of great technological importance in the design of welding alloys. It simply means that TRS can be relaxed in welded joints through transformation plasticity.

LTT alloys are being developed for the welding of high strength steels. Up to this time, there is no commercially known LTT alloy for multipass welding. This is probably because no definite, proven conclusion that cuts across many conditions is available on the structural integrity of joints welded with these alloys. The benefit of LTT alloy in a multipass welding of thick plates, typical of practical engineering structures has not been fully established for different grades of steels. Most practical studies have been to establish the beneficial effect of the LTT on FS. The current LTT alloys have high alloying contents of Cr, Ni and in some design Mn. These alloys are used to lower the ά start temperature ($Ms._T$) of the WM. The fundamental property of LTT is that the γ should transform at low temperature, so that CRS is generated down to room temperature. But the composition generates hard microstructure and may promote precipitation of brittle carbides. High hardness can delay the formation of fatigue crack, but it is detrimental to toughness. This is partly because, increase in hardness reduces ductility and reduction in ductility impacts toughness – the ability of the joint to absorb energy before fracture. To solve this problem, studies on the smart combination of conventional welding alloys having good toughness and the LTT alloys have been reported. This paper reviews the design, application and results of the efforts in using LTT alloys in mitigating TRS, distortion and cracking in welded steel components. It also discussed areas where performance data are required.

The design of LTT welding alloys

The extent of usefulness of welded high strength steel in structural application will depend on the availability of welding consumables with matching mechanical properties. As the strength of the steel increases, the toughness tends to decrease (Grong and Matlock, 2013). The LTT alloy commonly have high strength, and this makes it attractive for welding high-strength steels. If good LTT welded joints can be made, this will allow the use of high-strength steels in engineering structures to reduce weight and conserve steel resources. The tendency for ά phase to increase sample volume influences the RS state of the material (Jones and Alberry, 1977) (HKDH. Bhadeshia, 2002). In other words, the transformation expansion that occurs when the γ transforms to ά tends to determine the level of RS mitigation in the weld (Satoh et al., 1966) (Satoh, 1966). Formation of ά can be influenced by alloying elements such as C, Si, Mn, Ni, Mo, Cr, W, Ti, Nb and V. Chromium (Cr), Si, and Mo are known ferrite, α stabilisers and C, Mn and Ni, γ stabilisers. They can strongly affect the stability of the γ and the α since their solubilities are not the same in the two phases. Understanding the temperature at which ά occurs is vital in the design of LTT alloys. In fact, is the prime factor in the design of LTT welding alloys. The knowledge enables metallurgists to adjust transformation free energies to obtain different volume fractions of other phases, e.g. retained austenite (γ_r), to vary

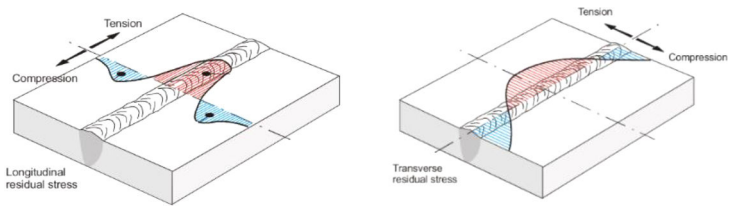

Fig. 1. Schematic of RS orientation and magnitude in the (a) longitudinal, (b) transverse directions (Zerbst, 2020) (Orr, 2008).

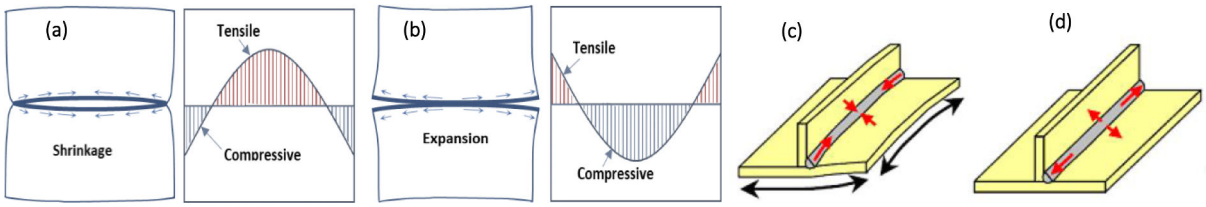

Fig. 2. The effect of tensile and compressive residual stresses along a longitudinal section of a weld (A Ohta et al., 1999) (Alghamdi and Liu, 2014).

mechanical properties of martensitic steels. Fig. 3 shows the effect of γ and α stabilisers on the $Ms._T$ of Fe-X binary system. The result shows that the effect is non-linear as the atomic percentage or solid solution of the alloying element increases. For a multicomponent steel, the trend is expected to vary. Clear and important information from Fig. 3 is that increasing alloying elements such as Al and Co will increase the $Ms._T$, hence undesirable. The target in weld alloy design is to increase the C, Mn, Cr, Ni, Mo, N and control the concentrations with regards to the impact on mechanical properties to obtain the desired final product. Though Cr is an α stabiliser, increasing its content was found to decrease the $Ms._T$ (Izumiyama et al., 1970) (Peet, 2014) (Capdevila et al., 2002) (Shirzadi et al., 2009), but it also prevents complete austenitisation at high content (Shirzadi et al., 2009).

The extent of the ά formation can also be influenced by the grain size and deformation of the prior γ (Yang and Bhadeshia, 2009) (Heinze et al., 2013) (Yang et al., 2012) (Shiga et al., 2010). It is found that large γ grain size increases hardenability, while fine γ grain size would provide many heterogeneous sites, increasing the chances of other phases to nucleate. Martensite, ά phase is hard, but brittle due to the excessive carbon content in interstitial solid solution. To obtain good combination of strength and toughness, it is commonly tempered to allow the excess carbon to precipitate as carbides. At relatively low tempering temperatures, cementite/iron carbide (Fe_3C) is formed and the hardness or strength of the ά is decreased. If the steel contains strong carbide forming elements such as Mo, Cr, Va, Ti, and W, at temperatures above say 500 °C, carbides of these substitutional elements such as Mo_2C, Cr_2C, Mn_2C, etc. can precipitate at the expense of the Fe_3C (Thomson, 1992), leading to what is referred to as secondary hardening (Igwemezie et al., 2016). In general and following a decreasing order, elements C/*N*>Mn>Ni>Cr>Cu>Mo>Si can decrease the $Ms._T$ while Al>*V*>Ti>Co>Nb>*W* can raise the $Ms._T$ (Izumiyama et al., 1970). Nb, Si and W were found to have small or negligible effect on the $Ms._T$. Other studies (Izumiyama et al., 1970) (Li et al., 2021) reported that V, Ti and W can decrease $Ms._T$ in a multivariate system.

Carbon (C) stabilizes γ relative to α and increases hardenability. But high levels of carbon may lead to formation of hard and brittle ά upon cooling. In stainless steels, formation of brittle carbides/Cr carbide can occur after welding leading to corrosion susceptibility and cracking. These defects lead to unacceptable reductions in part toughness. In the presence of RS, brittle ά can encourage hydrogen-assisted cold cracking and short fatigue life. Hence, low carbon and nitrogen in weld fillers is reported to be beneficial in reducing hard and brittle ά. To improve toughness, carbon content in the welding alloys is kept low. Hence, conventional LTT alloys designed to have low $Ms._T$ relied heavily on Cr, Ni and Mn to increase hardenability and to obtain acceptable mechanical properties.

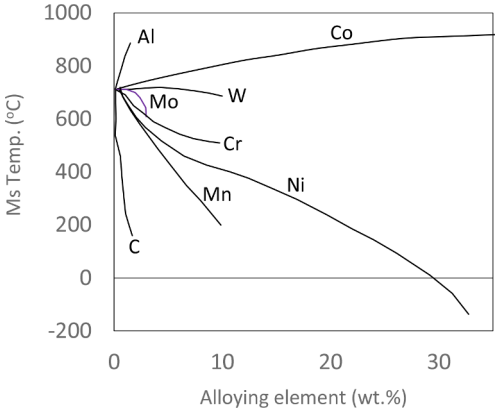

Fig. 3. The effect of γ and α stabilisers on the ά-start temperature ($Ms._T$) of steel (Izumiyama et al., 1970) (Peet, 2014).

Since the pioneering work on RS relaxation by ά transformation in a constrained body (Jones and Alberry, 1977), there have been many studies on LTT alloy based on the theory. (Ota et al., 2000) (A Ohta et al., 1999) (A Ohta et al., 1999) (Ota et al., 2001) (Ohta et al., 2003) designed a welding alloy named 10Cr-10Ni to improve the fatigue performance of welded joints by reduction of the TRS. Fig. 4 is the common graphs that have appeared in many publications to show the comparison of the developed alloy with a conventional welding wire.

The study fundamentally assessed the variation of the strain (ε) or stress (σ) on the longitudinal axis ε_y as the alloy cool down to the ambient temperature (T_a). Fig. 4(a) shows the ε in WM under condition of free deformation or unconstrained cooling. The ε vs. temperature (T) is plotted. For the conventional wire, during the cooling small expansion occurred around 500 °C. The material experienced the expansion when γ transformed to ά which stopped at the end of the transformation. As the material continued to cool down, it contracted further down to the T_a. The ε_s denotes the amount of shrinkage from the $Ms._T$ to the T_a. The $Ms._T$ for the 10Cr-10Ni was reported to be around 180 °C. The transformation started and completed just close to the T_a so that the WM was in a state of expansion at the final state. The ε_e denotes the amount of expansion from the $Ms._T$ to the near T_a. Fig. 4(b) shows a situation where the material was prevented from shrinking during cooling. As the constrained material cools down, thermal contraction leads to build up of TRS in the vicinity of the welded joint. For the conventional weld alloy, after the completion of the ά transformation, the TRS built up rapidly and progressively towards the T_a with a value approaching 400 MPa. For the 10Cr-10Ni, the ά transformation led to development of CRS down to the T_a such that the longitudinal strain was cancelled. In this experiment, the extent of the CRS induced by the ά expansion depicted how well it counteracted the TRS in the constrained joints.

An interesting LTT study was carried using martensitic steel (9Cr1Mo), bainitic steel (2.5Cr1Mo) and austenitic steel (AISI 316). A portion of the sample was heated to the γ phase and allowed to freely expand and then constrained and allowed to cool down to the T_a. As the constrained material cools down, thermal contraction led to the build-up of TRS as shown in Fig. 5. The figure shows that ά transformation occurred at about 500 °C for the 9Cr1Mo steel as indicated by the sudden drop in the stress value. The 2.5Cr1Mo transformed to bainite (α_b) at about 600 °C, also resulting to a drop in the stress level. As usual, there is a general RS relaxation that occurred during the displacive transformations. The RS reduction is higher for the 9Cr1Mo than the 2.5Cr1Mo steel. This implies that ά formation relaxed contraction stress more than α_b. Fig. 5 also shows that as the cooling continued to the T_a and after the displacive transformation is completed, the stress again built up eliminating the effect of the prior transformation stress relaxation. The Fig. 5 includes the insertion of the YS of the γ as a function of

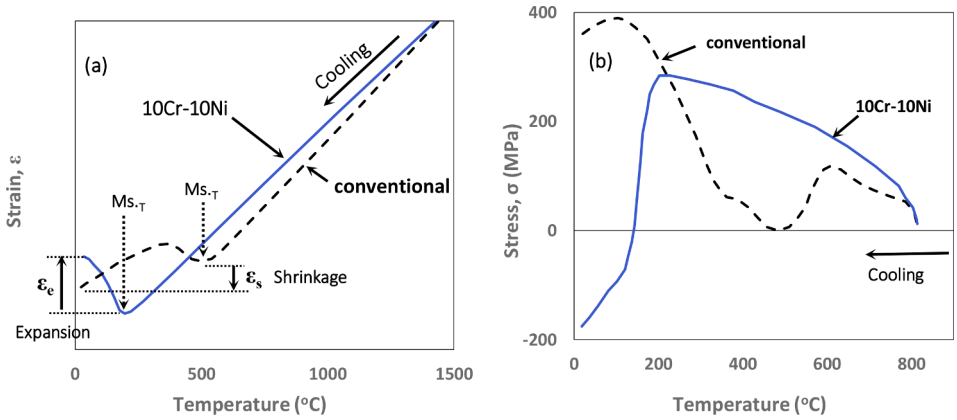

Fig. 4. The change of residual strain/stress with temperature for LTT and conventional weld wires: (a) strain and (b) stress (Ota et al., 2000) (A Ohta et al., 1999) (A Ohta et al., 1999) (Ota et al., 2001) (Ohta et al., 2003) (Miyata and Suzuki, 2015).

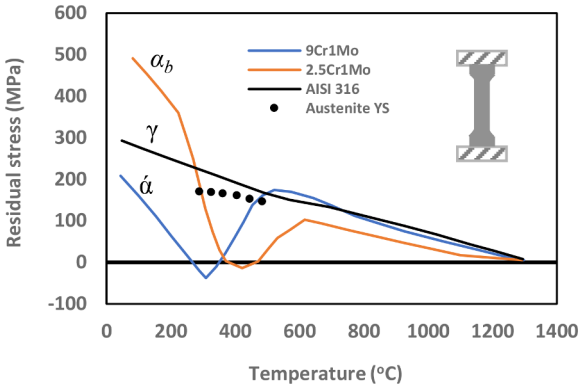

Fig. 5. Stress changes during cooling in uniaxially constrained samples (Bhadeshia et al., 2007).

temperature (Bhadeshia et al., 2007). This indicates that the YS of γ is lower than that of α at low temperatures. During thermal contraction, γ can yield or deform plastically to relax the strain due to its low strength, but α will elastically accommodate more strain. The higher strength of α resulted in lesser counteraction of the accumulating contraction strains by plastic relaxation, leading to higher TRS (Bhadeshia et al., 2007). This tends to explain why the stress increased rapidly towards a higher value for the α_b after transformation.

For the AISI 316 steel, martensitic or bainitic transformation was absent, hence the TRS simply continued to build up to the T_a, but the value is less than that of α_b. The TRS is significantly higher in the α_b. One of the challenges therefore is to transform the phases at low temperatures else the TRS state may be worsened (JA Francis et al., 2007).

Fatigue strength (FS) of structural steel joints welded with LTT alloy

As aforesaid, design of LTT is commonly centred on reducing TRS, improving FS and reducing distortion associated with welding without additional post weld heat treatment. From the discussions in Section 2, after LTT welding, the weld beads are expected to expand during cooling to the T_a to relax the TRS. (Ohta et al., 2003), compared the FS of 10Cr-10Ni and YGW24 fillers on a SM570Q base plate.

The dilatation test performance extracted from their work is shown in Fig. 6(a) and the RS build up is shown in Fig. 6(b). The chemical compositions and other properties of the wires are given in Table 1. Fig. 6(a) shows almost similar trend in YGW24 and SM570Q steels. Fig. 6(b) shows that high TRS was induced in both YGW24 and the base metal, while significant CRS occurred in the 10Cr-10Ni alloy. The FS comparison of the 10Cr-10Ni with conventional welding alloy in a lap joint was carried out. The weld was on a thin steel plate (JIS SPFH 590) of 2.3 mm thickness with a welding wire diameter of 1.2 mm. The material properties and the welding conditions were as given in Table 1 and Table 2 respectively. The differences in welding conditions were attributed to the variations in electrical resistance and viscosity between the two wires. Fig. 7(a) shows the S-N curves for a single lap joint welded with the two welding wires. It is very clear that the FS of the 10Cr-10Ni is superior with a fatigue limit of about 475 MPa while that of MGS-63B welding wire is about 300 MPa. This fatigue improvement has been attributed to the stress ratio effect and differences in the effective stress range. The addition of the TRS peak to the fatigue test load increased the

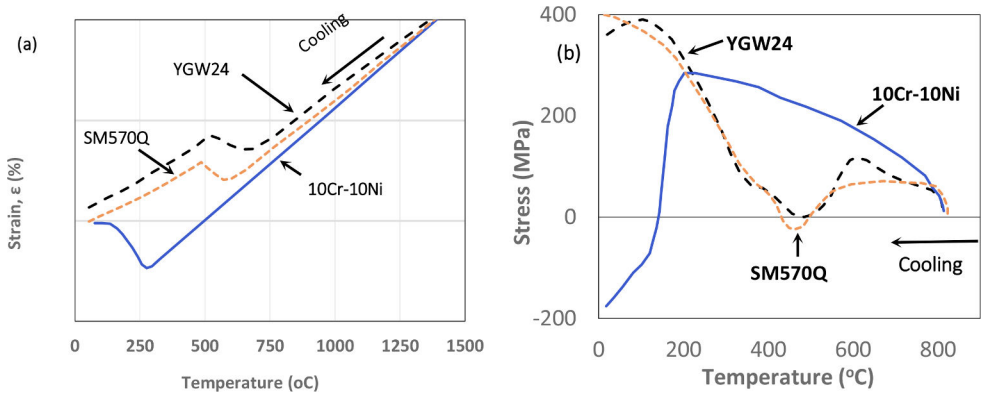

Fig. 6. The change in strain or stress during cooling (Ohta et al., 2003) (Suzuki et al., 2004).

Table 1
Chemical, transformation and mechanical properties of welding wires discussed in this study.

Weld Alloys	Chemical composition (wt.%)						Transformation properties		Mechanical properties		
	C	Mn	Si	Mo	Cr	Ni	~ $Ms._T$/°C	ε_f (%)	YS	TS	El (%)
Conventional											
MGS-63B (YGW24) (Ohta et al., 2003)[47]	0.08	1.09	0.5	0.29	0.42	–	590 −678	−0.51	580	660	29
SM570Q (Ohta et al., 2003)	0.12	1.29	0.24	0.06	0.03	0.02	569	−0.41	579	644	34
KC60 (Ota et al., 2000)	0.07	0.96	0.49	0.42	–	–	450	−0.23	579	661	27
KM80 (Ota et al., 2000)	0.06	1.21	0.20	0.48	0.80	2.66	444	0.02	760	810	25
Ok Autrod 12.51 (Eckerlid et al., 2003)	0.10	1.10	0.70	–	–	–	500	–	–	–	–
XY (A Ohta et al., 1999)	0.13	1.86	0.03	0.53	–	–		–	–	–	–
OK Autorod 89 (Ooi et al., 2014)	0.09	1.90	0.80	0.60	0.30	2.20		–	–	–	–
Filarc PZ6119 (Eckerlid et al., 2003)	0.06	1.1	0.4	0.3	–	2.9		–	–	–	–
Miki, et al. study (Miki et al., 2012)	0.09	0.65	0.25	–	0.61	0.6	600	–	470	570	–
OK 75.78 (Moat et al., 2011)	0.05	2.00	0.19	0.60	0.40	3.10	388/400	–	1000	–	–
308LSi (Moat et al., 2011)	<0.03	1.8	0.8	<0.3	20.3	10.0	–	–	–	–	–
LTT											
10Cr-10Ni (Ota et al., 2000)	0.025	0.70–1.09	0.32	0.13–0.29	10.0	10.0	180	0.55	882	1192	26 or 7
B206 (WM) (OK Tubrod 15.55) (Eckerlid et al., 2003)	<0.01	1.8	0.4	2.5	12.5	6.7	–	–	~717	~792	–
13Cr/LC35 (WM) (Eckerlid et al., 2003)	0.04	0.8	0.5	2.2	12.3	7.3		–	~743	~799	~15
LTT-C (Ooi et al., 2014)	0.014	1.27	0.70	0.07	13.4	6.10	281	–	–	–	–
LTT-S (Ooi et al., 2014)	<0.02	<2.00	<1.00	<2.00	15/18	6 −8	221	–	–	–	–
Miki, et al. Study (Miki et al., 2012)	0.06	0.25	0.17	–	–	10	350	–	808	852	–
OK Tubrod 15.55 (Barsoum and Gustafsson, 2009)	0.01	1.80	0.40	2.50	12.5	6.7		–	–	–	–
MX-4AD (Miyata and Suzuki, 2015)	0.03	4.30	0.38	–	–	–	472	–	727	820	23
LB-3AD (Miyata and Suzuki, 2015)	0.03	3.30	0.41	–	–	3.30	408	–	895	973	20
LTTE (Miyata and Suzuki, 2015)	0.07	1.30	0.20	–	9.10	8.50	200		1135	1287	6
Series B (JA Francis et al., 2007)	0.03	0.50	0.65	0.50	1.00	12.0	275	–	1100	–	–
Ok 84.52 (Moat et al., 2011)	0.16	0.37	0.73	0.06	12.9	0.05	250	–	–	–	–
Camalloy (Moat et al., 2011)	0.01	1.5	0.73	0.06	13.0	6.0	216/ 280	–	838	–	–
CamAlloy 4 (Moat et al., 2011)	0.01	1.36	0.74	0.10	12.66	5.24	–	–	–	–	–
CamAlloy 5 (Moat et al., 2011)	0.01	1.64	0.64	1.03	12.90	5.84	200	–	–	–	–
Base plate											
HT580 (Ota et al., 2000)	0.14	1.41	0.31	<0.01	0.04	0.05	460	- 0.06	497	605	34
HT780 (Ota et al., 2000)	0.10	0.85	0.17	0.50	0.48	1.25	440	- 0.05	821	821	31
Domex 700 (Ota et al., 2000)	0.06	10.85	0.07	0.08	0.05	0.06		–	709	778	23
SPV490 (A Ohta et al., 1999)	0.12	1.22	0.28	0.11	0.01	0.02	–	–	–	–	–
Miki, et al. Study (Miki et al., 2012)	0.15	1.53	0.38	–	0.01	0.03		–	439	556	25
Weldox 960 (Moat et al., 2011)	0.20	1.60	0.50	0.70	0.70	2.00	370	–	960	–	–

YS – Yield strength (Mpa), TS – Tensile strength (Mpa), EL – Elongation (%), WM – weld metal, ε_f - Strain.

Table 2
Welding parameters for MGS-63B and 10Cr-10Ni (Ohta et al., 2003) (Miki et al., 2012).

Weld Alloys	Welding parameters Shielding gas – 80%Ar+20%CO_2 @2.5 L/min			
	Current (A)	Voltage (V)	Welding speed (mm/min)	Heat input (kJ/cm)
MGS-63B (YGW24)	150	18	750	2.20
10Cr-10Ni	170	22	700	3.20
Miki, et al. study	130	10–11	200.5	4.19

stress range for the conventional alloy leading to poor fatigue performance. For the 10Cr10Ni, the CRS that resulted from phase change reduced the contraction strains. It was reported that the CRS was induced around the weld toe of the lap joint which led to crack propagation resistance leading to significant improved fatigue life.

(Ota et al., 2000) compared the FS of box welded joint using 10Cr-10Ni and some other conventional welding alloys (KC60 and KM80) listed in Table 1. Included in the table is the strain values, ε_f. KC60 was used to weld HT580 steel plate and KM80 for HT780 steel plate. The welding was performed in three passes. All the passes were allowed to cool to the T_a at the same time from a temperature above the $Ms._T$. Fig. 7(b) shows the fatigue performance of the box-welded joints. The fatigue limit of the HT580 steel welded with the conventional alloys was reported as 65 MPa while that of 10Cr-10Ni was around 130 MPa. This was almost twice the fatigue limit of the conventional alloys. The FS of out-of-plane gusset HT780 specimen welded with 10Cr-10Ni was again studied by (Ota et al., 2001). He found that the FS was almost three times higher than conventional weld filler. The improvement was still attributed to the CRS induced by the LTT alloy.

(Eckerlid et al., 2003) assessed the impact toughness, static mechanical strength, and fatigue properties of another developed LTT weld alloy named B206 (OK Tubrod 15.55) and 13Cr/LC35 using a thermo-mechanical rolled steel base plate named Domex 700. The property of the steel is given in Table 1. The microstructure of the base plate is reported to consist of fine α grains with small amount of pearlite and bainite.

The 13Cr/LC35 electrode was found to give an impact toughness of 50 J/cm^2 at −20 °C and B206 also fulfilled this requirement. However, increase in the number of beads reduced the impact toughness for the 13Cr/LC35 alloy. The performance of these LLT alloys were compared with those of Ok Autrod 12.51 and Filarc PZ6119 whose compositions are also given in Table 1 and the impact toughness also fulfilled the 50 J/cm^2 at −20 °C requirements. They found that the weld alloy improved FS of box-welded joint by 25 to 90% at 2 × 10^6 cycles. Multipass weld was made with 100 °C interpass temperature (T_i) with welding details listed in Ref (Eckerlid et al., 2003). The fatigue test results for the joints are given in Fig. 7(c). The figure showed improvement of the FS with the use of the LTT alloys against the conventional ones. The improvement tends to increase with decrease in the fatigue stress level. These LTT electrodes were reported to reduce the TRS significantly, particularly at the weld toe. But the CRS shifted the point of crack initiation from the weld toe to the weld root. Their tests suggested that the number of beads and the type of stress waveform could affect the fatigue result. It also indicated that fatigue peak load could relax the beneficial CRS thereby reducing the effectiveness of the LLT alloys.

Another interesting comparison of conventional welding alloy OK

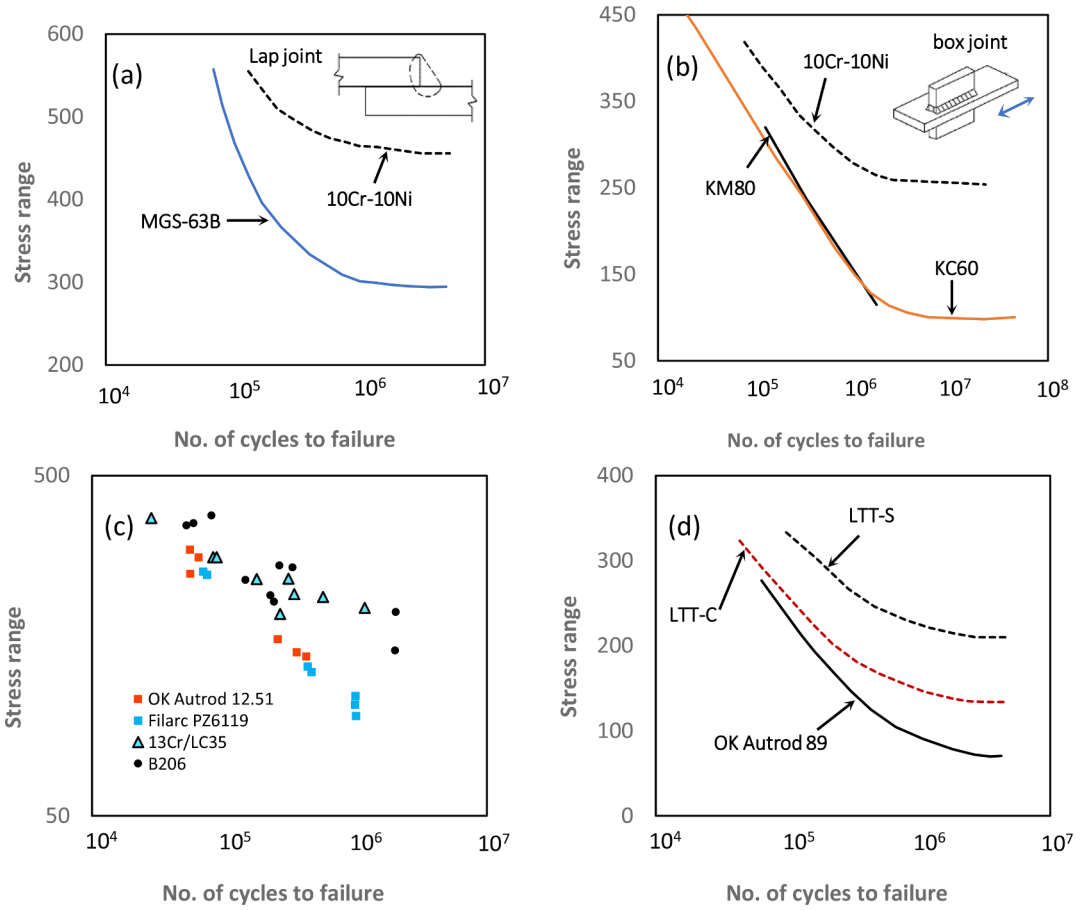

Fig. 7. The fatigue strength test comparison of LTT with conventional welding alloys.

Autrod 89 and LTT-C, LTT-S alloys is shown in Fig. 7(d) (Karlsson and Mraz, 2011) (Ooi et al., 2014). The experiment was conducted to assess the FS of a single-pass fillet welds. The compositions and the transformation properties of these alloys are shown in Table 1. The FS of the LTT alloys is clearly higher and the fatigue limit of the LTT-S is about 3 times higher than that of the conventional one. If all other factors are constant, we can conclude that the fatigue life was improved due to reduction of TRS in the joint welded with the LTT filler. Later studies by (Bhatti et al., 2013) using LTT-C and LTT-S wires on a longitudinal stiffener fillet welded joints showed that FS was improved in the modern steels. (Barsoum and Gustafsson, 2009) compared OK Autrod 12.51 (conventional) wire with OK Tubrod 15.55 (LTT) with compositions given in Table 1. They found that FS of the LTT was significantly higher than that of conventional wire under constant amplitude, but the CRS induced by the LTT alloy was somewhat relaxed under spectrum loading, thereby reducing the FS.

Recently, (Hensel et al., 2020) studied the FS of LTT welded joints of S355J2 steel and high strength steel S960QL base plates. The alloy was reported to be martensitic with no γ_r. This was compared with some conventional filler materials. The conventional wire had required impact toughness but low FS while the LTT had high FS, but low toughness. Hence the study focused on combination of the two wires to obtain joint having both toughness and good fatigue resistant. They investigated the stability of RS in a box-welded joints of S355J2 and S960QL under quasi-static and fatigue loading. LTT filler was applied as an additional weld bead to a circumferential conventional bead. The LTT filler was applied only around the areas prone to fatigue crack initiation – such as the weld toe at the end of the welded longitudinal stiffeners. They measured RS in the as-welded condition and after the quasi-static and fatigue loadings. Under tension loading, they found that the RS was stable in the high strength steel S960QL up to 350 MPa as shown in Fig. 8 (a) and RS relaxation and re-distribution occurred in the S355J2 when the load increased to 240 MPa as shown in Fig. 8(b).

For the fatigue loading with stress ratio of $R = 0.1$, load = 400 MPa, the RS was reported to be stable again in S960QL up to 100,000 cycles as shown in Fig. 8(c). An increasing RS relaxation with load cycles was observed in the S355J2 as shown in Fig. 8(d). Generally, the CRS tended towards TRS state in the S355J2. This result implies that the CRS benefit of LTT alloy can vary for different steel grades under similar service loading conditions. They also reported substantial increase in FS with the use of the LTT alloy as shown in Fig. 9. For the S960QL V-groove and DY-groove butt weld, fatigue crack or failure point was observed at the weld root with the use of the LTTW (Fig. 9(a)). Failure point was observed from the weld toe for DY-groove joint for the conventional wire. This result tends to show that the use of LTT alloy shifted the fatigue start point from the conventional weld toe to the weld root. This suggests that while CRS is induced around the weld toe by the LTTW, the equilibrating TRS may have shifted to the root area. Though, the authors attributed the shift to the weld root to lower stress concentration caused by smoother weld toe angle of the LTT weld metal (LWM). FS of V-groove LTTW joint was significantly higher than that of DY-groove LTTW or conventional joint. In other words, DY-groove welded with LTTW has the lowest fatigue resistance.

Comparison of the DY-groove welded with conventional and LTT fillers tends to show that failure from the weld toe is less severe than failure from the weld root. This indicates that the type of joint can strongly affect the performance of LTT alloy. For the box-welded component in Fig. 9(b), the fatigue crack initiation was observed at the weld toe for both the conventional and LTTWs. The LTT weld generally increased the FS, but the highest strength was obtained in the

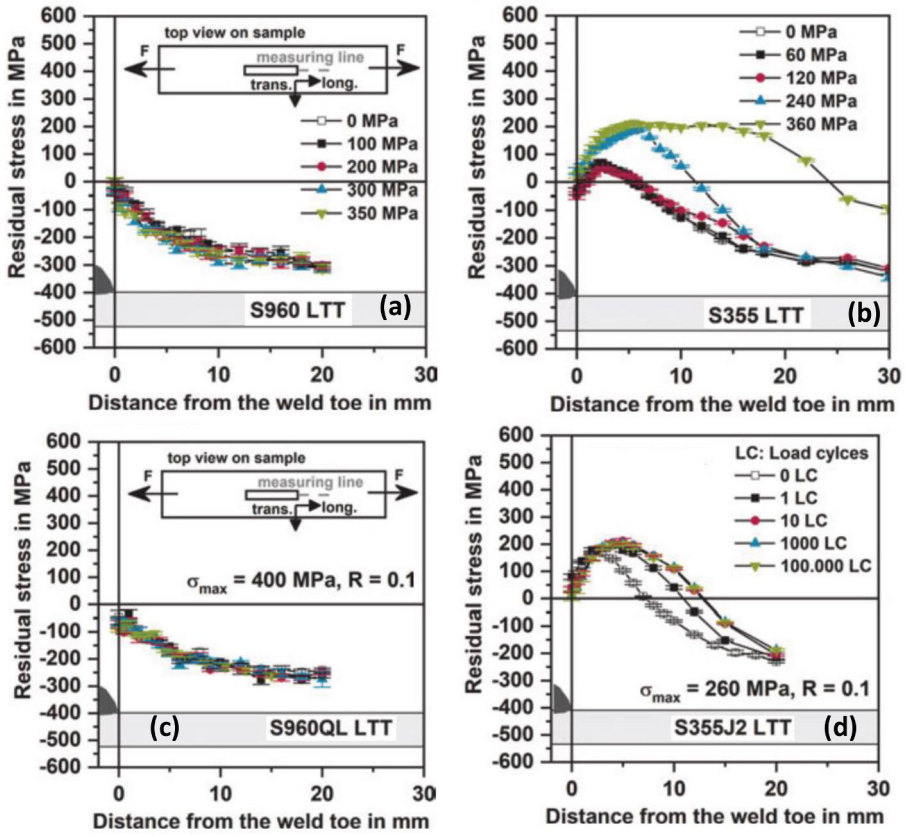

Fig. 8. Transverse RS at the weld surface of S355J2 and S960QL (a) RS stability in S960QL under tension loading, (b), RS relaxation in S355J2 under increasing tension loading, (c) RS stability in S960QL under fatigue loading, (d) RS relaxation in S355J2 under fatigue loading in Hensel, et al. study (Hensel et al., 2020).

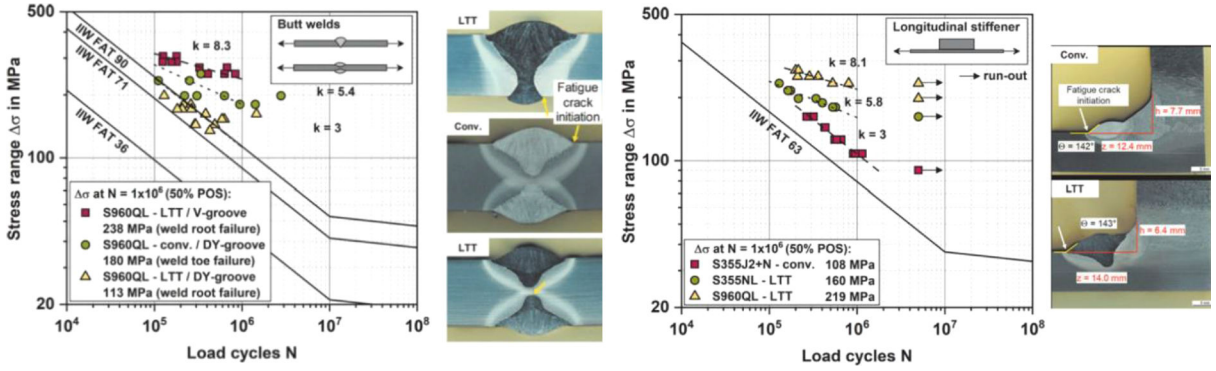

Fig. 9. Fatigue strength results in (Hensel et al., 2020) study with macrographs of butt and box welded samples showing fatigue crack nucleation sites.

S960QL steel. (Hensel et al., 2020) attributed the increase in FS of S960QL as compared to the S355 steel to the stable CRS field and low TRS in the material. They informed that high FS observed in the V-butt welds could not be explained using the RS effect. In conclusion, the authors pointed out that there was no general mechanism of FS enhancement in the studied materials.

FCGR in structural steel joint welded with LTT alloy

The fatigue life of a welded component depends on the rate of propagation of existing weld flaws (cracks, undercut, lack of fusion, etc.) in the joint. The rate is naturally accelerated by the existence of TRS and geometrical irregularity introduced by the weld - causing stress concentration, typically at the weld toe and root (Karlsson, 2009). The sharper the geometrical transition between the weld and the base plate, the more the deterioration of the FS due to higher stress concentration. (A Ohta et al., 1999) compared the FCGR of joints on a SPV490 steel plates welded with 10Cr-10Ni and a conventional wire named here as XY. A machined centre notch through the butt WM specimen as show in Fig. 10(a), was used. The compositions of the materials are given in Table 1.

The RS distribution along the width ($W = 200$) of the sample is shown in Fig. 10(b). In the figure, conventional WM induced a TRS in the middle area, reaching up to about 91 MPa at about 35 mm from the centreline of the sample width. Fig. 10(b) also shows that the TRS was almost eliminated, and CRS induced in the middle region using the LTTW. However, at the edges the equilibrating RS was compressive for the conventional wire (reaching up to 303 MPa) and tensile with a peak up to 89 MPa for the LTT WM (A Ohta et al., 1999). The experimental FCGR data are shown in Fig. 10(c). The result clearly showed that the

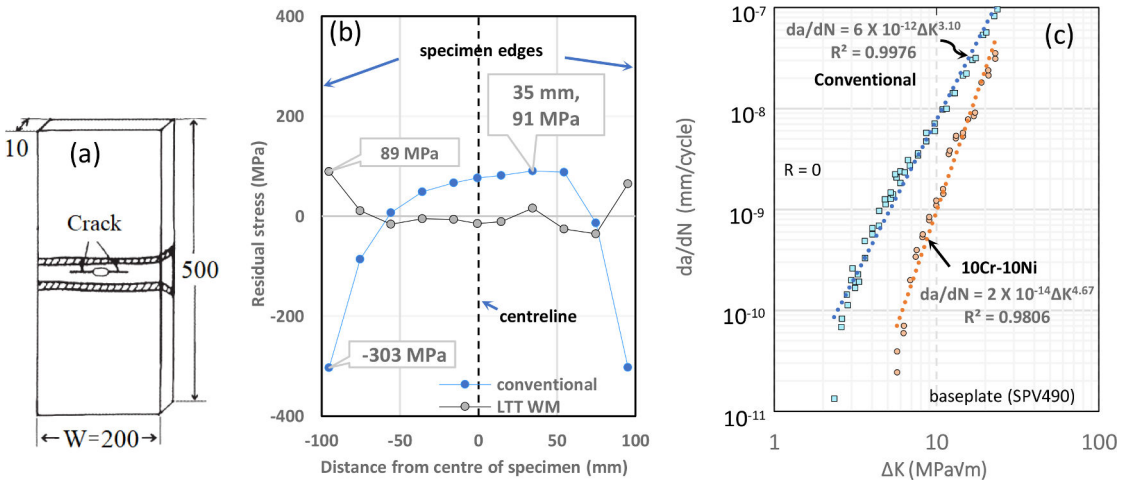

Fig. 10. The fatigue crack growth comparison of LTT and conventional welding alloys (A Ohta et al., 1999).

reduction of TRS in the LTT joint decelerated the rate of crack growth considerably in comparison with the XY alloy. Although, the sample welded with LTTW was reported to have received heat treatment at about 720 °C and cooled in air. This heat treatment, due to uniform heating and cooling has the potential of relaxing RS in the surrounding materials. Hence, may not represent as-welded condition. In this sense, the fatigue crack propagation performance of the welding alloy may not be attributed entire to the LTTW transformation. Nevertheless, this experiment clearly emphasized the detrimental effect of RS on the FCGR of welded structures.

FCGR in high strength steel repaired with LTT alloy

(Miki et al., 2012) carried out an interesting study on the benefit of using LTTW in the repair of cracked joint of plate girder. They assessed FCGR and the re-distribution of the compressive stress field introduced by the LTT weld repair on the crack propagation behaviour. They used gouging and re-welding of the gouged zone method in the repair assessment of α-pearlite steel of YS and TS of 439 MPa and 556 MPa respectively. The other properties of the steel and that of the consumables are listed in Table 1 and the welding condition in Table 2. Fig. 11 (a) shows the configurations of the experimental CT-specimen and WM layering technique in their study (Miki et al., 2012). TIG welding was used as it was reported to be suited to weld repair than other methods. In their study, they allowed the crack that initiated from the machined notch to propagate up to 20 mm. At this crack length, the cracked area was gouged and repaired by welding with the LTT and conventional wires. Note that the repairs LTT #1 and LTT #2 were made with the same wire. The gouged specimen was restrained by clamping before welding.

The effect of RS (redistribution) as fatigue crack propagated was evaluated using strain gauges. The initial RS distribution appeared to be obtained by sectioning the sample and the values of the released strains noted. Fig. 11(b) shows the initial RS distribution from the top side of

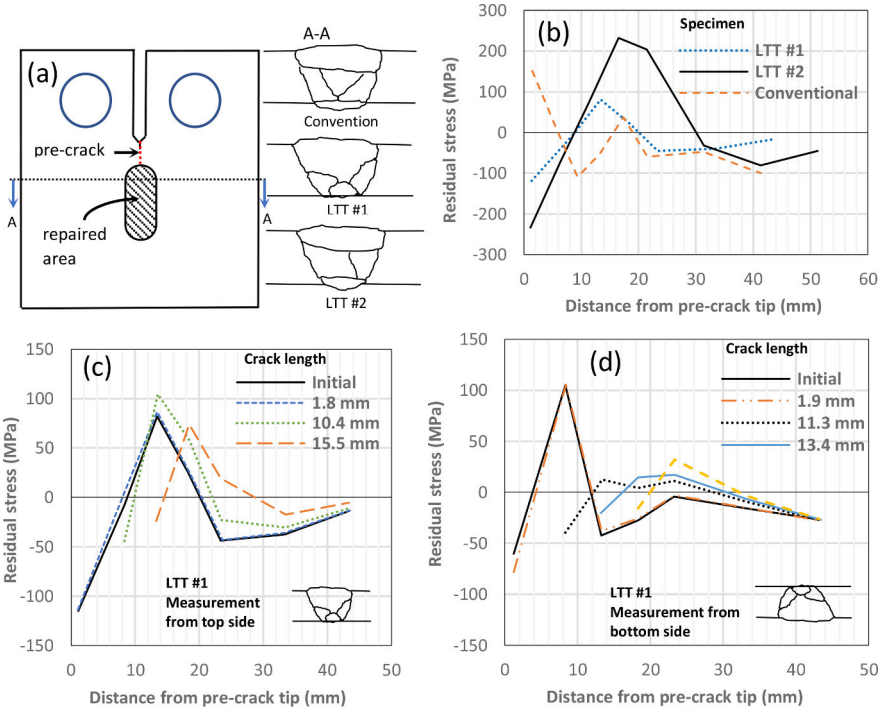

Fig. 11. The sample configuration, weld repair method and stress distribution in (Miki et al., 2012) study.

the weld. As the fatigue crack propagated during the test, the residual strain was released and this value was measured periodically. The difference between the initial value of the released strain and that during the crack propagation was used in evaluating the RS re-distribution. In Fig. 11(b), it is interesting to note that though the repairs LTT #1 and LTT #2 were made with the same wire, the RS distribution differed. LTT #2 had high CRS in the vicinity of the pre-crack tip that extends up to 9 mm, but the middle section of the weld up to 27 mm was mainly tensile, with peak stress above 200 MPa. In comparison, the LTT 1 had less compressive stress and considerably less tensile stress, with peak below 100 MPa, in the mid-section of the weld length. It then appears as if reduction in pre-crack tip compressive stress reduces the tendency for high TRS peak in the mid-section of the weld. This difference may have arisen from the multi-layer weld deposition strategy. In other words, deposition strategy may be a factor to be quoted in evaluating the performance of these LTT alloys. The conventional wire, as expected, had TRS in the vicinity of the pre-crack tip up to about 6 mm and the rest is largely compressive. One would have expected substantial tensile stresses in the mid-section, but that was not the case. The equilibrating force appeared to have induced the CRS at a distance from the TRS field. Fig. 11 (c & d) show the comparison of the initial stress distribution (solid line) and the redistribution of the RS from the top and bottom of the weld of bead length of about 28 mm - as the crack propagated through the LTT #1 weldment. The values varied from the top side of the weld to the bottom side and this was attributed to the layering of the weld passes. In other words, the laying technique affected the RS distribution.

Fig. 12(a) shows an interesting observation from the crack tip radius measurements of samples repaired with the welding wires. Note that the WM is constrained by the surrounding baseplate while the notch end by virtue of the crack opening was free to move, especially inwards from WM shrinkage or outward from WM expansion. After the repair weld, the tip radius reduced from the initial machined notch tip radius of 0.079 mm. The reductions before repair and after repair are shown below the images in Fig. 12(a). It was reduced by 0.034 on average for the LTTW and 0.052 for the conventional wire. In other words, the reduction in the tip radius was larger for the conventional wire. This tends to suggest that the shrinkage in the conventional weld pulled close the initial crack tip opening thereby making it sharper. Sharp crack tip will accelerate the crack initiation process. For the LTT weld, the expansion resulting from the phase change encouraged less sharpening of the crack tip. Therefore, the displaceable end of the C(T) may have some effect on the RS distribution in the samples – especially close to the pre-crack tip.

Fig. 12(b) shows the reported FCGR through the base metal before repair and through the LTT weld metal (LWM) after repair. The growth pattern of the base metal somewhat differed from that of the WM. The compressive stress from the LTT weld tends to improve or extend the initial crack propagation life. In other words, higher stress or more cycles at a particular stress intensity level are needed to advance the propagating fatigue crack in the LWM. But as soon as the crack traversed the compressive stress field crack growth rate could become rapid. In other words, the Paris region may be very steep. This may be the case for the LTT #2 weldment. LTT #2 had the highest CRS and TRS peak in the middle section. The compressive stress may have retarded the crack initiation, propagation rate, but after traversing this field the rate became very rapid. In other words, having high CRS at the weld toe may not necessarily mean that the structure is safe to operate. The rate at which the crack will propagate may have to be evaluated. The rapid growth rate is not desirable as engineering structures are expected to fail in a safe manner. Paris-curve angle of slope should be low for a fail-safe design.

It must be noted that generally, the CRS value decreased as the crack propagated as shown by Fig. 11 (c & d). The disparity in the values of stress re-distribution between the top and bottom sides can be attributed to the variation in the weld beads deposition. In other words, the weld beads deposition strategy affected the RS distribution in a LTT weld joint. This tends to be supported by the disparity in the FCGRs for the LTT #1 and LTT #2 weldment in Fig. 12(b). Also, since the RS reduced as the crack grew, the disparity between the crack growth rate before repair (base metal) and LWM cannot be attributed wholly to the CRS. Because even the conventional wire was compressive in the middle of the weld. In other words, the effect of LTT alloy on the FCGR may be eliminated at a distance exceeding about 6 mm. The WM properties, including the microstructural phase morphologies and texturing may be one of the factors contributing to the differences. In general, these early studies showed clearly that the LTT alloys performed better than the conventional filler alloy and that FS can be improved without post-weld heat treatment – particularly for few mm steel samples.

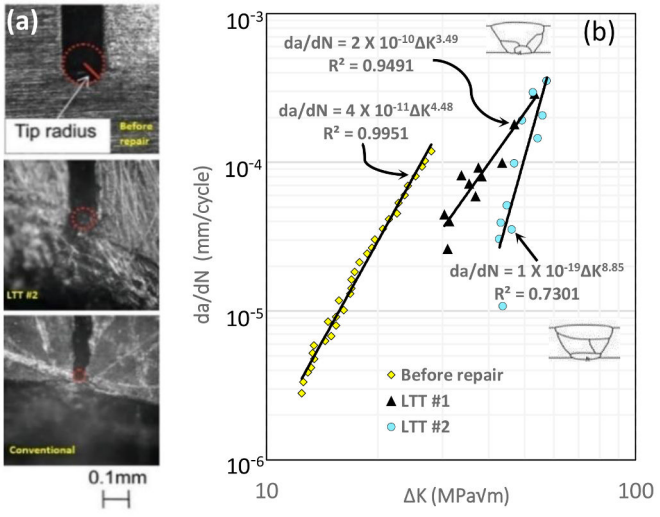

specimen	Machined notch (Before repair)	LTT wire		Conventional wire
		#1	#2	
Crack tip radius (mm)	0.079	0.051	0.040	0.027

Fig. 12. (a) Nature of crack tip before and after weld repair, (b) FCGR of the base metal and repair weldment.

FCGR in high strength steels welded with LTT alloy

(Hensel et al., 2015) also studied the influence of TRS field on a FCGR in S355J2+*N* steel of YS = 440 MPa, TS = 560 MPa and S960QL steel of YS = 1010 MPa and TS = 1075 MPa. The crack propagation and the redistribution of the TRS was observed. They varied the mean stress, $(\sigma_{max} + \sigma_{min})/2$, and the RS state in the sample. The result of the stress ratio $R = 0$ is discussed here as it is more damaging of the cases considered. The specimens were clamped to induce the RS and samples were tested under as-welded and stress-relieved conditions. The thermal stress-relieving was done for 30 min at 600 °C (S355J2+*N*) and 570 °C (S960QL) respectively. They used x-ray and neutron diffraction methods to determine the state of the RS at the vicinity of the crack tip as the crack propagated. The cyclic stress amplitude was reported as 130 MPa using sinewave of 20 Hz. The welding did not involve any filler wire. Table 3 shows some of the results obtained from the fatigue test for the $R = 0$. For the S355 steel, the effect of the thermal stress-relieving on the FS is little. But the number of cycles to failure for the S960QL weld was considerably reduced by the thermal stress-relieve. Ordinarily, one should have expected the stress relieved S960QL welded sample to have higher FS due to some reduction in the TRS, but this was not the case. The stress relieving heat treatment rather deteriorated the fatigue life of the S960QL. This result is similar to the crack growth results they obtained, which is presented in Fig. 13.

Table 3 shows the fatigue test results generated in the (Hensel et al., 2015) study. For S335J2+*N*, the number of cycles required to propagate the crack in the as-welded was less than that needed for the stress-relieved sample. This is expected as TRS must have been reduced in the stress-relieved sample. For the S960QL, large difference was observed in the number of cycles needed to propagate the crack. The crack growth in the as-welded condition is surprisingly slower than that of stress-relieved condition. That is, the number of cycles needed to propagate the crack is higher in the as-welded condition. In other words, reduction of TRS in the S960QL welded sample by stress-relieving heat treatment had no effect on crack growth or it adversely affected the crack growth resistance. The result then suggests that the heat treatment may have altered the microstructural properties of the S960QL which deteriorated the fatigue properties (Hensel et al., 2015). Or defects in the form of brittle carbides may have been precipitated in the microstructure during the heat treatment of S960QL that deteriorated the fatigue growth resistance.

(Hensel et al., 2015) also presented stress relaxation result as the crack propagates in the weld. The measurements were taken after unloading the samples. For the S355J2+*N* steel under stress-relieved condition, the initial RS was compressive at the crack tip, but with value close to zero. At 3 mm, the compression at crack tip increased and TRS of about 50 MP was recorded in front of the crack tip. At 6 mm, the compression at the crack tip increased further close to 200 MPa and the TRS in front of the crack tip decreased to a value less than 50 MPa. For the as-welded condition, the notch tip was also in compression up to 100 MPa and TRS of about 200 MP was observed ahead of the crack tip (in the vicinity of the HAZ). At 3 mm from the notch, both CRS and TRS values decreased to about 100 MP. At 6 mm, the CRS at the crack-tip increased and TRS up to about 50 MPa generated in front of the crack tip. For the as-welded sample S960QL, CRS was recorded at the crack tip and TRS of over 250 MPa observed at a distance in front of the crack tip. At crack length of 3 mm, the CRS only changed slight as the crack propagated and the TRS ahead decreased to about 200 MPa and shifted into the baseplate. At $a = 6$ mm, the TRS disappeared, and the crack tip remained in compression. This experiment shows that at unloaded condition, the tip of a propagating fatigue crack is generally in compression while the TRS decreases and shifts in front of it as it grows. They also found that change in the mean stress led to variations in the fatigue life. They concluded that in welded structures RS was reduced when the sum of the RS and load stresses overcome the yield strength of the material. Also, that re-distribution of RS occurs as fatigue crack propagated. This study confirms that the RS state of a body containing crack relaxes and redistribute as the crack grows.

Table 3
Fatigue tests in (Hensel et al., 2015) study.

$R = 0$ sinewave = 20 Hz		As-welded	Thermally stress-relieved
Material	Stress amplitude	Load cycles to failure	Load cycles to failure
S355J2+*N*	130 MPa	40,800	44,920
S960QL	167 MPa	74,232	28,227

Design of LTT alloy to prevent cold cracking in high strength steel

Increase in carbon-equivalent of the WM increases hardness and joint restraint affects RS. Diffusion of hydrogen can cause embrittlement. The tendency for cold cracking increases as these factors increase. A good LTT alloy should be able to reduce TRS, prevent cracking, improve fatigue life and depending on the environment resist corrosion. (Zenitani et al., 2007) presented an interesting report on the development of LTT weld alloy to prevent cold cracking in high strength steel welded joints without pre-heating treatment. The LTTW was designed to have microstructure containing ά and retained austenite (γ_r). The γ_r is an austenitic phase that did not transform to ά after cooling from high temperature to the T_a. The γ_r is expected to help absorb or trap hydrogen and prevent cold cracking under high joint constraints. The dilatation curve for the conventional wire and the LTTW used in their study is shown in Fig. 14(a). The conventional weld alloy has a strength of 780 MPa and transformation from γ to ά or α_b started at about 436 °C and ended around 327 °C. Further cooling to the T_a at the end of the transformation causes WM to contract further thereby inducing TRS in the WM. The LTT alloy during the transformation expanded down to the T_a and inducing a CRS. The ε and $Ms._T$ were reported to be measured at a cooling rate of 20 K/s from 1573 K (≈1300 °C) by dilatometry (Zenitani et al., 2007). Table 4 shows the chemical compositions of the WMs obtained for the three weld wires - A (LTT), B (martensitic stainless-steel rod) and C (800 MPa class steel rod).

The average diffusible hydrogen content in the WMs were reported as 5.33, 5.72 and 6.00 mL/100 g respectively. The dilatation tests for the WMs are given as shown in Fig. 14(b). From Table 4 it appears that increase in Cr, Ni to some extent Mn were the major changes used in reducing the $Ms._T$. Fig. 14 (c, d & e) show the microstructures of the WMs and Fig. 14(f) is the macrographs of the y-groove weld-cracking-tests (Tekken test) performed on the WMs. Major cracks were reported in the B and C while minor crack was observed in A. The disparity in the hydrogen contents in these WMs was seen as contributing little or nothing to the cracking results. The microstructures of A and B were similar and martensitic. Their HV values were above that of C that was reported to have mixture of ά and α_b. Therefore, the cracking resistance in A was not attributed to the microstructure, but to the reduction of TRS by the ά transformation. It then appears that increasing hydrogen, C and Si and decreasing Ni and Cr contents made the WM susceptible to cracking. The alloy A was then modified by increasing γ_r in the microstructure to reduce the diffusible hydrogen in the WM, since γ has higher solid solubility of hydrogen than ά. The resultant WM from the modification is labelled D and the composition and other properties are shown in Table 4. Observation shows that Mn, Si and Cr were slightly increased in the modified alloy. The γ_r was increased from about 0% in the WM A to about 12.7% and this appeared to have decreased the HV from 366 to 313 and the $Ms._T$ to about 94 °C from 210 °C (Zenitani et al., 2007). Fig. 14(g) shows the $Ms._T$ of the WMs and their effect on the RS. The RS decreased and became compressive as the $Ms._T$ is decreased. The alloying composition of A appeared to give the maximum CRS. Despite the high CRS in A as compare with D, cracking was reported to be absent in D. Zenitani, et al. (Zenitani et al., 2007) then concluded that γ_r is an

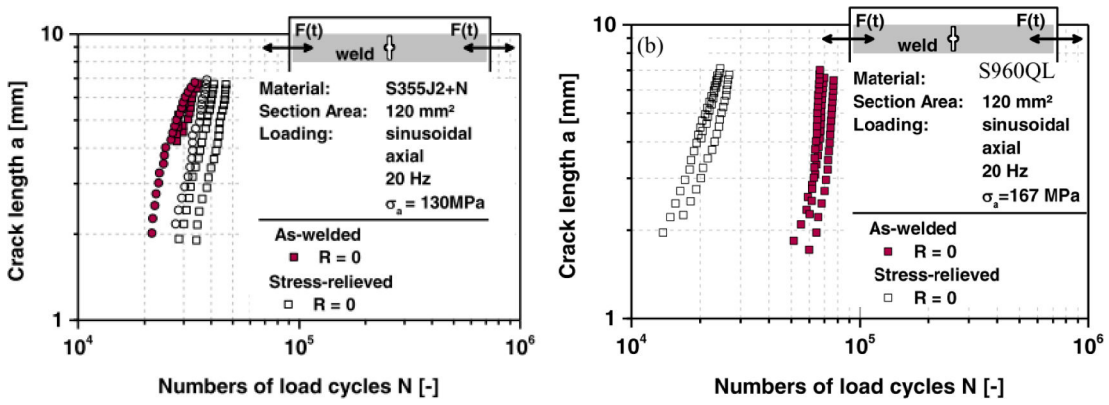

Fig. 13. Fatigue crack growth results in (Hensel et al., 2015) study.

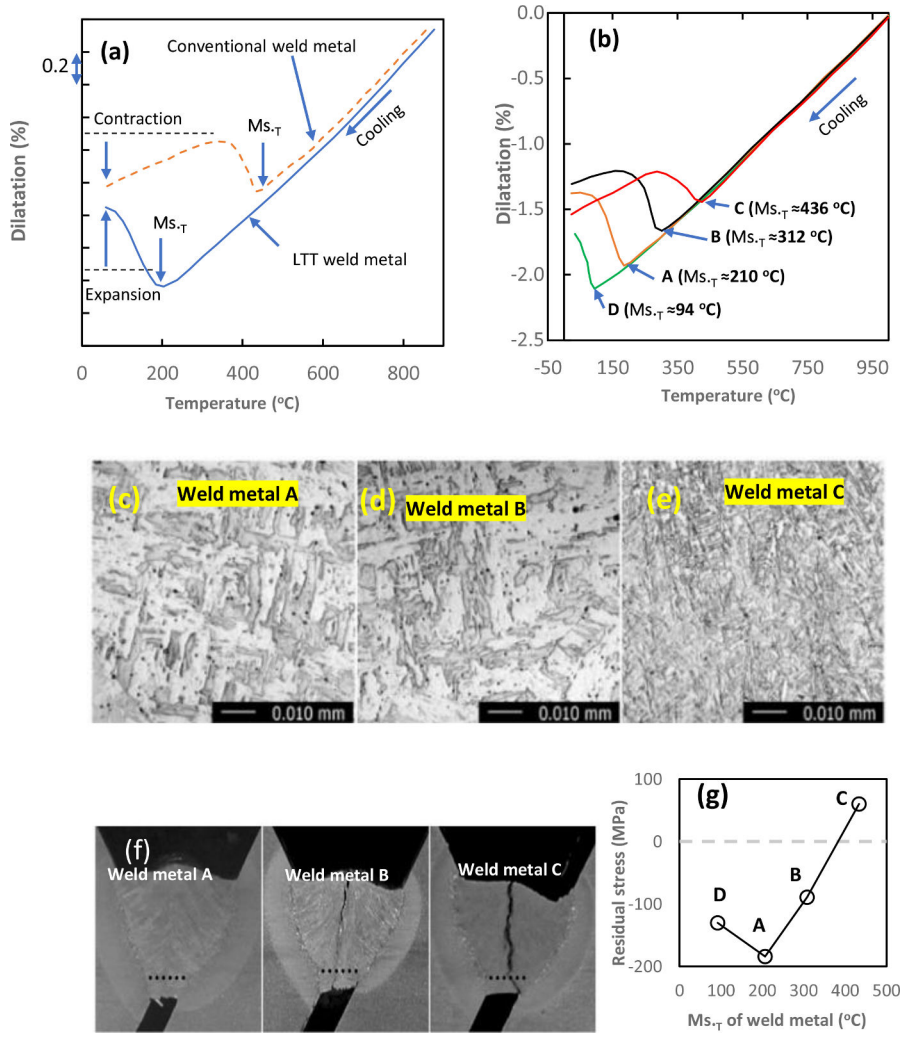

Fig. 14. The properties of conventional and LTT welding alloys in (Zenitani et al., 2007) study.

important factor in preventing cold cracking in addition to the CRS induced by the LTT alloys. In their conclusion, a LWM having microstructure consisting of ά and γ_r phases could prevent cold cracking without the need to preheat the weld joint.

Limitations of Cr, Ni LTT welding alloys and commentary on Mn-LTT alloy design

Table 1 and Table 4 show that most of the 'conventional LTT' weld alloys are designed using high Cr and Ni contents to lower the $Ms._T$. This makes the weld alloy consumables very costly. The use of high Ni can unnecessarily increase the strength of the weld beads in comparison with the base metal. This increase in strength may deteriorate the

Table 4
WMs chemical composition (wt%) in (Zenitani et al., 2007) study.

Weld metals	Chemical composition (wt.%) of weld metals									
	C	Mn	Si	Mo	Cr	Ni	$Ms._T$ (°C)	γ_r (%)	H diffusivity (mL/100 g)	Hardness (HV)
A	0.05	0.73	0.25	0.30	10.10	8.80	210	–	5.33	366
B	0.07	0.55	0.28	0.40	9.90	4.40	312	–	5.72	386
C	0.09	1.18	0.52	0.31	0.60	1.76	436	–	6.00	334
D	0.05	1.50	0.40	0.30	11.10	8.60	94	12.7	–	313

cracking resistance of the weld joint and could make the WM brittle. The use of Mn reduces cost, but martensitic Fe–Mn alloys have been found to be brittle (Bolton et al., 1971). This was attributed to segregation of Mn and P to the boundaries of the prior γ (De Souza et al., 2005). (Miyata and Suzuki, 2015) presented an appealing report on the development of LTT weld alloy that exploited Mn in lowering the $Ms._T$. The starting alloy for the design was a conventional weld alloy named MX-200. The Mn and Ni contents of the base alloy were increased as shown in Table 5 for FCW B and FCW C while only Mn was increased for FCW D and E. Fig. 15 (a, b & c) show how conventional and LTT welding alloys were combined to produce tough joints in the (Miyata and Suzuki, 2015) study. Fig. 15(a) is welded with conventional weld alloy only, Fig. 15(b) with LTT alloy only and Fig. 15(c) with the combination of conventional and LTT weld alloys. The conventional was observed to have good toughness, but low FS due to the TRS at the weld root and toe. The crack resistance in the LWM was reported to be poor, but the FS is improved due to the existence of the CRS. For the conventional and LWM combination joint, the crack resistance was said to be good, and the FS was improved due to the CRS induced by the LWM at the weld toes.

The three-point bending fatigue test results on the joints made with the weld wires are shown in Fig. 15 (d, & e). The fatigue performance of the joint improved with increase in the Mn or Ni additions, but Mn appeared to have performed better than Ni. In other words, the study showed clearly that Mn can suitably replace Ni in designing effective LTT alloys. Based on these results, the compositions were slightly adjusted to meet practical toughness requirements leading to development of two Mn alloys named MX-4AD and LB-3AD with properties as given in Table 1. Fillet joints were made with MX-200 and the weld toe treated with MX-4AD, LB-3AD, peening and grinding. The three-point bending fatigue test results of the joints in comparison with other fatigue improvement methods are shown in Fig. 15(f). The figure showed that the joint treated with LB-3AD (with about 3% Mn and 3% Ni) offered the highest resistance to fatigue. In other words, the use of the LWM as additional weld beads could improve the FS more than improvement of weld toe fatigue resistance by grinding or peening.

Further studies on LTT alloys

Generally, the intention of LTT alloy improvement is to produce tough joint with reduction or elimination of TRS and resistance to hot/cold cracking. One of the reported issues with the 10Cr10Ni is that it lacked sufficient impact toughness (Charpy impact energy of just 20 J at 20 °C which limited its structural application (Moat et al., 2011) in marine environment. (JA Francis et al., 2007) compared the performance of three fillers - OK 75.78 (a standard ferritic filler), LTTE and Series B, with wide $Ms._T$; 388 °C, 200 °C and 275 °C respectively. Unconstrained tensile specimens of the alloys were heated to 850 °C. After the austenitisation, the specimens were then fixed rigidly and allowed to cool to the T_a at a rate of 10 °C/s. The result is shown in Fig. 16(a). As usual, the ά transformations in the LTTE and Series B resulted to CRS on the samples. LTTE had the highest compression followed by Series B. For the OK 75.78, after the completion of the ά reaction at about 349 °C, the TRS rapidly built up to T_a. They used single pass weld on Weldox 960 baseplate to compare their ability to reduce harmful TRS. They confirmed that lower $Ms._T$ resulted to less damaging TRS distribution in the vicinity of the fusion zone and HAZ.

Table 5
Composition of welding wire in (Miyata and Suzuki, 2015) study.

Weld wire	Mn	Ni	Ms (°C)
MX-200 (base)	1.7	0	670
FCW B	2.1	3.1	490
FCW C	2.0	5.2	390
FCW D	3.6	0	490
FCW E	5.5	0	310

(Moat et al., 2011) in their study appeared to have extended the work of (JA Francis et al., 2007). They designed two alloys. They used conventional ferritic wire (Wang et al., 2002) as the starting point for their first alloy (Series b -which is essentially the same as Series B in Francis, et al. study). OK84.52 (conventional martensitic stainless welding alloy) was used as the starting point for their second alloy (Camalloy) for austenitic stainless steel. Two strategies used by Moat, et al. in their modelling to lower $Ms._T$ was to either reduce the fraction of α stabilisers (Cr, Si, Mo) or increase the γ stabilisers (such as C, Mn, Ni). They kept the Cr low in the ferritic case (Series b) and at minimum Cr content (12.9 wt.%) in the stainless case (Camalloy). The compositions of these alloys are shown in Table 1. The dilatation tests for their study are presented in Fig. 16(a). In Fig. 16(a), the ά transformation was completed at about 150 °C for the Series b and Camalloy at about 160 °C. The final RS in the Camalloy was about 20 MPa (tensile) and that of Series b is about −30 MPa (compressive). The performance of the new alloy was compared with others. Camalloy against 308LSi (conventional stainless fillers). The Series b was compared against OK75.78 (ferritic fillers) on Weldox 90 plates. The trial GMAW weld was made on a 12 mm thick grooved Weldox 960 plate using a single pass. The Camalloy was reported to have a finer martensitic microstructure. Both alloys were reported to have Charpy impact toughness of 27 and 53 J at −20 °C respectively which are acceptable for marine application. The Camalloy was observed to offer significant improvement in the fracture toughness of the joint. However, they were reported to introduce TRS below the fusion zone and such was not found using the conventional filler. But the TRS was said to be less than the TRS peak in the conventional filler in the longitudinal direction.

(Shirzadi, 2019) used thermodynamics calculations to model and design Camalloy 4 and Camalloy 5. The alloys were designed to mitigate TRS in stainless steel large weldments. The major improvement in these alloys tend to be the reduction of tensile stress peaks before ά transformations and the alloys had very low carbon content. The low carbon was desired to prevent precipitation of CrC_2 during welding as this carbide can reduce toughness. The Cr content was kept above 12 wt.% to maintain stainless properties, but not exceeding 13 wt.% perhaps because higher content can prevent complete austenitisation. The compositions of the alloys are shown in Table 1. The S and P contents were kept below 0.01to avoid hot cracking. The increased contents of Cr, Ni and Mo ensured that the alloy is fully martensitic upon cooling. Another concern considered is the hot cracking that occurs as high alloy WM solidifies. To avoid this, the molten weld needed to solidify as delta-ferrite (δ) first before transforming to γ. Solidifying wholly as δ was reported to prevent formation of low temperature melting peritectic that increases the susceptibility to hot cracking. It is also thought that small quantity of discontinuous δ in the microstructure of WM containing Ni can improve toughness. Fine γ grain size can contribute to

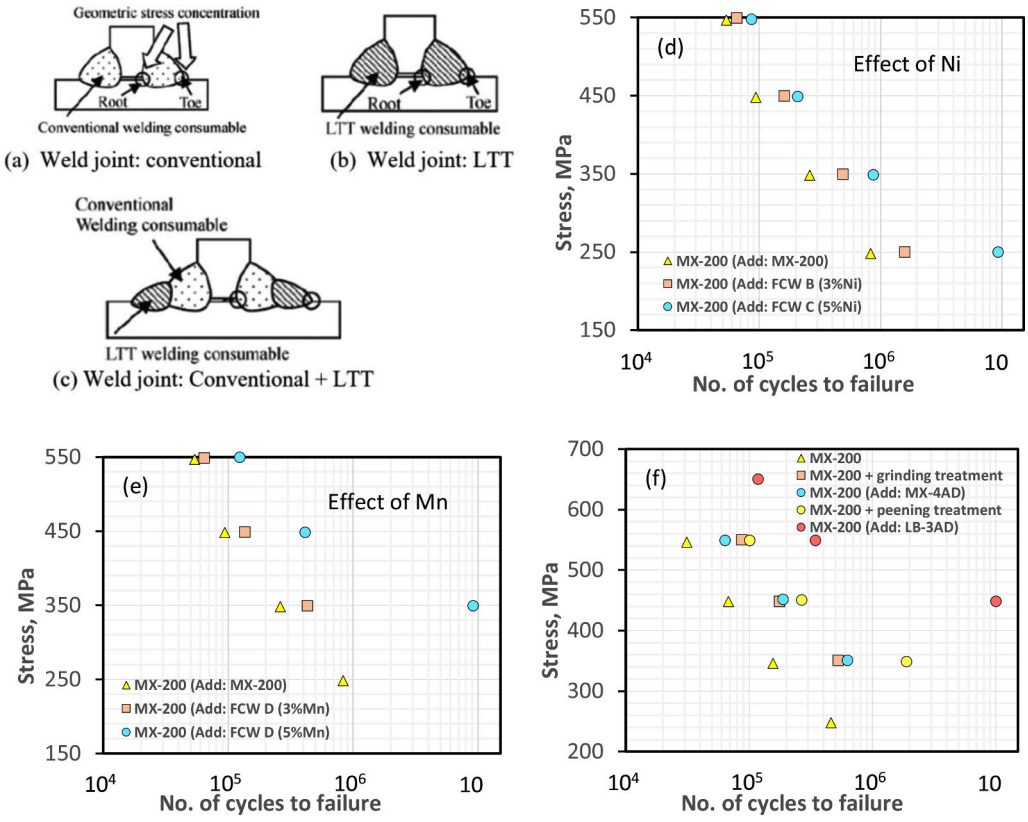

Fig. 15. Production of tough joints using conventional and LTT welding alloys (Miyata and Suzuki, 2015).

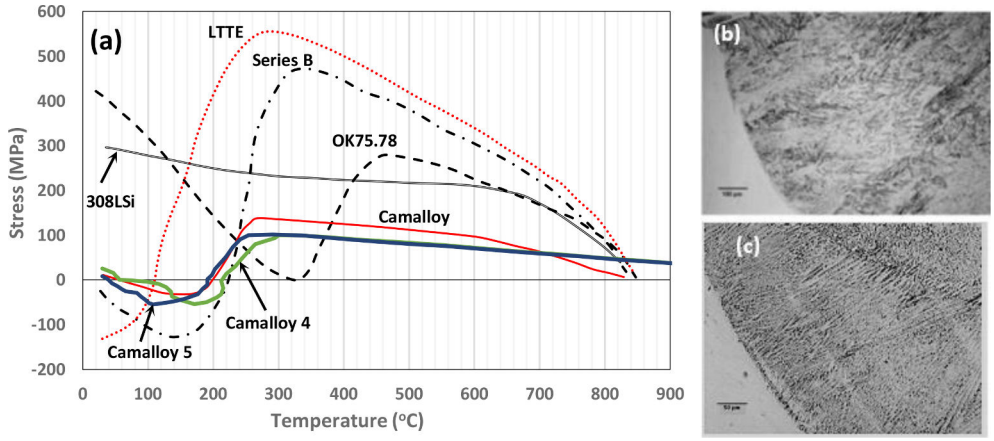

Fig. 16. LTT studies (a) Satoh test results in (JA Francis et al., 2007), (Moat et al., 2011) and (Shirzadi, 2019) studies, (b & c) Photomicrographs of designed welding alloys in (Shirzadi, 2019) study.

higher toughness. The γ grains are found to be finer if they transform from δ instead of transforming directly from the molten metal (Zhang and Farrar, 1995). This consideration can be found in the study of the effect of Ni on the columnar grain development of as-deposited C-Mn-Ni and C-Mn-Ni-Mo WMs carried out by (Zhang and Farrar, 1995). Fig. 17 shows the region of high temperature of Fe-Ni phase diagram. Fig. 17(a) shows the phase fields for the melt (L), δ and γ in Fe-Ni alloy system (Zhang and Farrar, 1995) . The domain that will guarantee that the melt solidifies as δ tends towards low alloying content. As the Ni content increases, this domain shrinks and above about 3.4 wt.% Ni, δ and γ phases will be present. How γ is formed now will depend on whether the composition is between 3.4 - 4.5 wt.% or 4.5 – 6.2 wt.% or above 6.2 wt. %. In the first case, immediately the temperature drops below the peritectic reaction line, molten metal already co-existing with δ will transform to γ. This results to two solid phases (δ and γ) of different crystalline structures having different compositions of Ni. As the temperature continues to drop, the δ will eventually transform to γ. The γ that formed later may contain increased Ni content. In the second case, at a very narrow band somewhere between 4.5 – 6.2 wt.% both the molten metal L and δ may transform to γ at the same time. Beyond this, the melt will co-exist with the γ and as the temperature drops, the remaining melt transforms to γ. This kind of solidification creates pockets of peritectic phases with differing alloying contents and areas of slightly differing melting points. This may encourage hot cracking. Fig. 17(b) shows the effect of increasing equivalent Ni (Ni_{eq}) content on the width of resultant γ columnar grains in the weldment. The figure

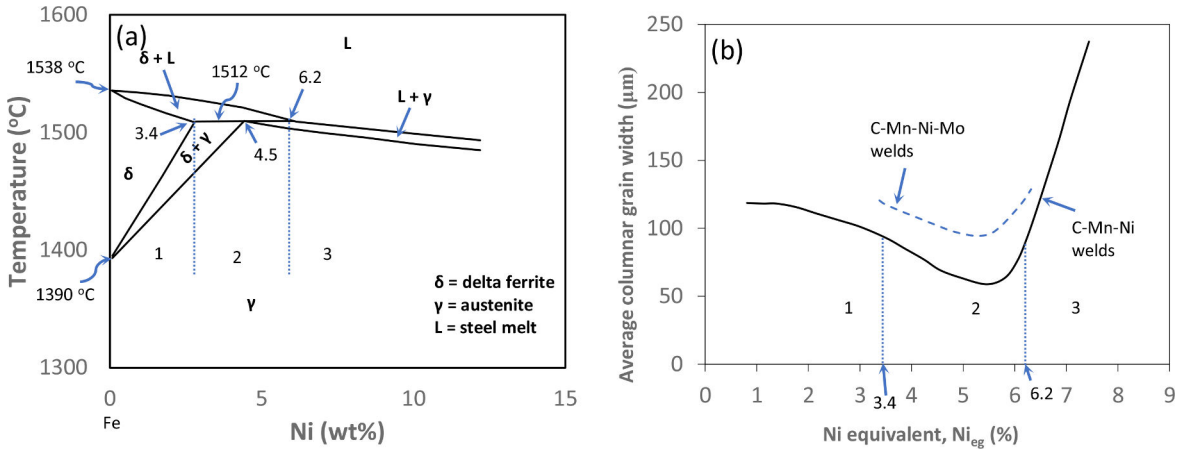

Fig. 17. Fe-Ni equilibrium phase diagram, (a) The peritectic (high temperature) region (b) effect of Ni_{eq} on the columnar grain width (Zhang and Farrar, 1995).

shows that beyond about 5.8% Ni_{eq}, the width of the columnar grain starts to increase. The article reported that the smallest columnar grain was obtained in the WM between 3.4 – 6.2% (region 2) and the largest width occurred at Ni_{eq} above 6.2% (region 3).

This is apparent in Fig. 17(a), as Ni_{eq} beyond 6.2% will result to simple epitaxial growth of the γ – i.e., continuation of γ growth in a preferred direction. This will produce WM with large columnar and fewer grains. From Fig. 17(b) then, initial increase in Ni_{eq} will refine the grains and as the Ni_{eq} increases a point is reached when thickening of the γ columnar grains occurs and continues with increase in the Ni_{eq}. Thus, the way γ is obtained will affect the final microstructural property from the γ → ά reaction. This constraint placed a limit on the use of the γ stabilisers like Ni in the design of welding alloys. The intention of (Shirzadi, 2019) in his study appears to be the adjustment of the alloying elements to achieve peritectic reaction of the form δ + L → δ, and then δ → γ and final γ → ά transform (region 1). In this way, the reaction will occur at different moments at various positions in the weld pool resulting to smaller columnar grains. The result of the Satoh tests on the Camalloy 4 & 5 designed by (Shirzadi, 2019) (Shirzadi et al., 2009) is also shown in Fig. 16(a). The weldment with Camalloy 5 was reported to have near zero distortion or less TRS than Alloy 4 in manual butt welding of a stainless-steel plates. Fig. 16(b) shows the microstructure of the Camalloy 4 at 100 μm and Fig. 16(c) the Camalloy 5 taken at 50 μm. The microstructures were reported to be almost entirely martensitic. Clearly, simply making the right adjustments in the alloying elements resulted in a finer ά plates in the Camalloy 5 and the retained δ-ferrite was reported to be present as a discontinued network. Small amount of discontinuous retained δ-ferrite has been reported to be beneficial to toughness (Shirzadi et al., 2009) while a continuous one deteriorates it. Despite the alloy did not induce the highest CRS amongst the alloys in Fig. 16(a), the microstructure of Camalloy 5 was reported to confer high toughness to the weld. This finding supports the observation in (Miki et al., 2012) that LTT with higher CRS may not be desirable for structural application. They suggested the use of the Camalloy 5 for a situation where it is difficult to carry out post-welding heat treatment. However, the use of expensive alloying elements in the design makes the welding wire costly. Hence, it was recommended for weld repairs and restoration process. (Moat et al., 2018) also studied the performance of the Camalloy 4 in a 8-pass groove weld of a 304 L stainless steel plate. They found that the TRS reduction capability of the alloy was reduced in a multipass weld. They stated that the interpass temperature (T_i) had a strong influence on the final state of the RS in the multipass weld. They then suggested the selection of T_i in the vicinity of the $Ms._T$. This is to delay the ά transformation until the weld sequence is completed. This would ensure that the whole weld zone transforms simultaneously. This they concluded would restore the ability of the alloy to reduce TRS.

(Harati et al., 2017) worked on the improvement of FS of high strength steel using LTT alloys. He compared his result with that of a conventional wire. One or two beads were used in their study. They associated low TRS in the joint to reduction of $Ms._T$ of the LWM. The FS of the LTT joint was reported to be 46% higher than that of the joint made with conventional filler. Highest FS was obtained for LWM with $Ms._T$ close to 200 °C. They stated that lowering the $Ms._T$ of the WM was more beneficial to fatigue strength than the specific combination of alloying elements. Since increase in Cr and Ni result to very low Ms.T, it implies from their conclusion that increasing these alloying elements would result to high FS in the weld joint of high strength steels. However, in welding stainless steel with alloy having high Cr and Ni contents, such a trend was not obtained. This again tends to show that the effectiveness of LTT welding alloy is material specific (see also (Hensel et al., 2020)).

(Hosseini et al., 2020) presented an interesting study of the effect of increasing Ni content of LWM on the RS developed in AISI 410 baseplate of 5 mm. The AISI 410 is a martensitic stainless steel which is hardenable – i.e., can be heat treated (quench and temper) to generate high strength with good ductility. It is often used where strength, hardness, wear resistance and some corrosion resistance are needed.

For the LTT, the Cr was kept constant at 11 wt.% and the Ni varied in the range 3 – 11 wt.% as shown in Table 6. Fig. 18 shows the increase in the Ni content and its effect on the $Ms._T$ and the final expansion strain (FES) of the LTT fillers and WMs in the (Hosseini et al., 2020) study. The figure shows usual trend of $Ms._T$ decreasing with increasing Ni. The higher value of the $Ms._T$ in the WM with respect to the filler was associated with dilution. Fig. 18 shows essentially that increased content of Ni did not translate to linear increase in the CRS in the WM. A maximum is seen in the values of the FES at about 7 wt.% Ni. Beyond this value, the FES decreased with increasing Ni. This downward movement was attributed to incomplete ά transformation at T_a. This result tends to show that the effectiveness of LTT alloy in mitigating TRS does not increase linearly with decrease in the $Ms._T$. Another study (Thomas and Liu, 2014) reported that LTTW containing 10Cr4Ni produced more CRS

Table 6
Cr and Ni contents of LTT fillers, conventional fillers and baseplate in (Hosseini et al., 2020) study with the calculated $Ms._T$.

Material	Element (wt-%) Cr	Ni	M_s (°C)
LTT1	11.34	2.95	269
LTT2	11.15	5.05	226
LTT3	10.86	7.12	179
LTT4	11.42	9.02	142
LTT5	11.05	11.24	60
ER410 (conventional)	11.5–13.5	0.6	301
AISI 410 (Base metal)	12.74	0.29	329

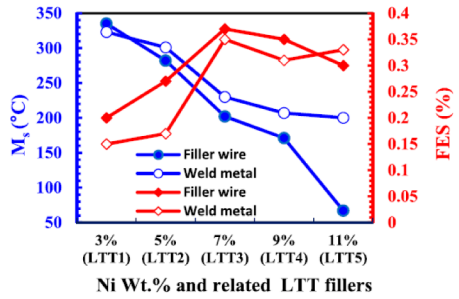

Fig. 18. The effect of increasing Ni content on the $Ms._T$ and final expansion strain (FES) of the LTT fillers and weld metals in (Hosseini et al., 2020) study.

than LTT alloys containing 1Cr10Ni. In a similar study, (Hosseini et al., 2021) stated that impact toughness was reduced by the presence of small amount of δ in the WM while γ_r improved the toughness.

Numerical modelling of LTT alloy

Some researchers have tried to understand the behaviour of LTT alloy through numerical modelling. (Novotný et al., 2016) in their numerical simulation of multipass welds using LTT alloy had already made similar conclusion as (Moat et al., 2018). They reported that use of T_i above the $Ms._T$ increased the effectiveness of LTT alloy under multipass condition. They stated that the transformation plasticity would be fully utilised if the temperature of the whole weld passes was maintained above $Ms._T$ before allowing the joint to cool to the T_a. They informed that the CRS was induced in the weld zone and its surrounding area. They also reported that the RS pattern was affected by alteration in the LWM transformation characteristics. (Jiang et al., 2018) in their experimental and numerical study also reported that high T_i, above the $Ms._T$, increased CRS in a multipass weld. (Z Feng et al., 2021) compared the benefit of LTT alloy over conventional welding wire on the fatigue resistance of a multipass welding of SM490A T- joint. The work involved experiment measurements of the RS developed in a T-welded joint. They also employed numerical method to confirm the result. They reported that in a multipass weld, the CRS in the previous bead could revert to TRS upon cooling if the reheating temperature from the subsequent pass was below the upper critical temperature (Ac_3). The area that was completely re-austenitised or above the Ac_3 upon cooling retained their compressive behaviour. He suggested that LTT alloys are better suited for a single pass welding. In another study, (Z Feng et al., 2021) reported that cooling rate and the coefficient of thermal expansion of the LWM effected the RS. He stated that more CRS was obtained with slow cooling and that FE analysis showed that plate thickness had a considerable influence on the distribution of RS in the WM. They also reported that LWM with $Ms._T$ of 191 °C was less sensitive to the joint size effect than the one having an $Ms._T$ of 398 °C.

(Wu et al., 2020) designed a LTT welding wire designated EH200B and compared its fatigue performance with that of a similar lap joint made with convention ER70S-3 wire. The lap joints for the fatigue test were made from DP980 steel panels and the study was on a single pass. Using FE model, they found that the part distortion patterns for the two wires were similar. The fatigue life of the LTT welded joint was found to be almost twice more than that of ER70S-3 and this was attributed to the reduction of the TRS in the weld and heat affected zones. (Choi et al., 2021) in their study compared the properties of Mn-based LTT weld with conventional weld and heat-treated conventional weld on a A516 steel plate. The LWM was reported to compose of α, γ, ά and α_b with phase fractions of 50.5%, 0.2%, 40.2% and 9.1%, respectively. The LWM was found to induce CRS in welded zone even more than that of the heat-treated conventional weld. (Wang et al., 2018) employed numerical and neutron diffraction to study the effects of chemical dilution and multipass welding on the effectiveness of LTT alloy. They concluded that multi LTT weld layers generated CRS, but the final state could be altered significantly. They also informed that dilution effected the formation mechanism of the RS. (Sun et al., 2020) in their study also reported that dilution could affect the RS distribution in a WM. (Wu et al., 2019) studied the toughening effect of γ_r in the LWM. They found that the impact toughness increased with increase in the volume fraction of the γ_r. They attributed this to the absorption of dislocations and transformation-induced plasticity (TRIP) effect of the γ_r. (Wu et al., 2018) also studied the performance of LTT filler in a single pass fillet welds. They reported higher CRS and improvement in fatigue strength for filler alloy with $Ms._T$ as low as 92 °C as compared with other LTT fillers with higher $Ms._T$ (183 °C). They also reported that dilution of the LWM by the Q345B base metal resulted to an increase in the Ms.T. Deng, et al. (Deng and Murakawa, 2013) through numerical modelling found that transformation-induced plasticity (TRIP) – resulting from the transformation of γ_r to ά due to application of stress could reduce TRS in the weld and heat affected zones, both in the longitudinal and transverse section. However, they stated that the effect was less than the effects of transformation volume change accompanying γ to ά transformation and the variation in mechanical properties resulting from the microstructure. The RS resulting from the LTT alloy has been explained in some way using the thermal expansivity of γ and α (Kromm et al., 2009). The γ is found to have more expansion per degree temperature increase than $\alpha/\alpha_b/$ά (Bhadeshia, 2004). This volume expansion would result to a greater counteraction of the accumulated thermal shrinkage in a constrained sample. During thermal contraction, γ can yield to relax the strain due to its low strength. As already mentioned, the volume fraction of the γ_r is a function of the chemical composition and solidification conditions (whether cooling is slow or fast). It then implies that the volume fraction of γ_r can affect the level of CRS induced by LTT alloys or the effectiveness of LTT alloys.

Microstructure and mechanical properties of LTT alloy

One thing many researchers did not include in their reports is the detailed microstructure of the investigated LTT alloy in as welded and stress relieved conditions. As aforesaid, a change in the LTT alloying compositions, will vary the $Ms._T$ and ά-finish temperature. This would produce different volume fractions of α, ά, γ_r and other phases that might be present. From the published data, the LTTWs commonly contains Ni in the range of 3 – 12%, Cr; 3 – 13%, while the $Ms._T$ can vary between 500 – 25 °C. Fig. 18(a) shows the $Ms._T$ as a function of Cr and Ni% only - neglecting the effect of the other alloying elements (Kromm, 2014) (Kromm, 2011). The temperature range plotted is 450 – 25 °C. The figure shows that the $Ms._T$ decreased with increase in Ni and/or Cr. Fig. 18(b) & (c) show the range of possible YS and TS of some reported LTT alloys as presented in Ref (Kromm, 2014) (Kromm, 2011). The YS is in the range of 300 – 1100 MPa and TS in the range 500 – 1300 MPa. Fig. 18 (b & c) show that the mechanical properties are deteriorated as the amount of Cr and Ni is increased in the LTT fillers. Increase in Ni content has more adverse effect on the mechanical properties. In other words, the mechanical property is controlled mainly by the Ni content. Since increase in Cr and Ni lowers the $Ms._T$, Fig. 18 (b & c) generally imply that reduction of $Ms._T$ using Cr and Ni is accompanied by reduction of YS, TS and consequently the impact toughness. Since Ni stabilises γ, it then appears that the increase in the volume fraction of the γ_r as Ni increases is responsible for the reduction in the mechanical properties. The figures show that increasing Cr to reduce $Ms._T$ is more favourable to mechanical properties than Ni.

(Kromm et al., 2011) studied the effectiveness of LTT alloys in multipass welding of thick samples and presented the microstructures of 10Cr10Ni LTT alloy in the as-welded condition as shown in Fig. 19. The weld microstructure is cellular - with primarily austenitic solidification as shown clearly in Fig. 19(a) (Kromm, 2011). The light etching was identified as the intercellular γ_r while the grey area is composed of fine ά. The cellular solidification produced columnar grains with network of

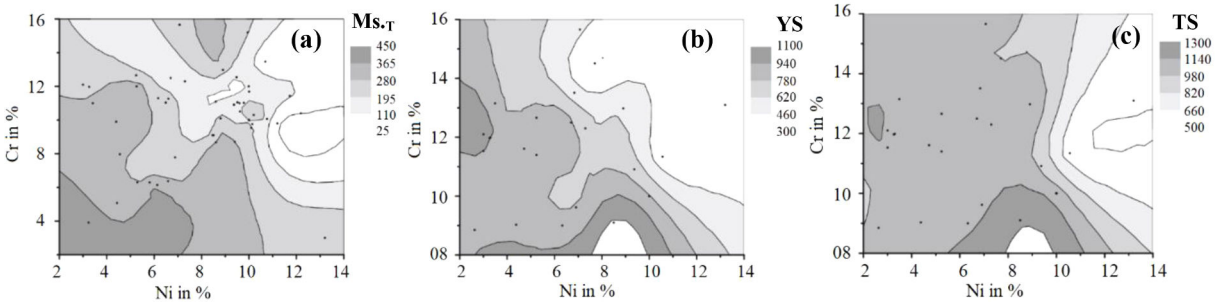

Fig. 19. The effects of increasing Cr-Ni on $Ms._T$, YS and TS of welding filler (Kromm, 2014).

γ_r (Kromm, 2014).

The γ_r in the intercellular areas was reported to solidify last because it contained higher amount of Cr and Ni in comparison to the grey areas. The high Cr and Ni in the γ_r network suppressed the ά formation in these areas to T_a. Fig. 19(b) shows that there exists a chemical gradient in the intercellular areas as indicated by the colour variation (Kromm, 2011). Cellular solidification allows alloying elements having low solubility in γ to segregate in the intercellular boundaries, forming low-strength film with a low melting temperature (McGuire, 2008). During contraction of weld pool under restraint, these perhaps brittle areas can crack. In Fig. 19(c), the arrows were reported to show solidification cracking in the γ_r intercellular network (Kromm, 2014). These cracks deteriorate the fatigue properties of the LTT weld alloy. Fig. 19(d) is the microstructure of 10Cr12Ni alloy showing fine ά. However, the dark and light etchings show that the alloying elements were not uniformly distributed. (Kromm, 2014) also reported that micro-segregation found in the intercellular areas of the LTT having high Ni can be eliminated by the re-heating of underlaying weld bead in a multipass weld. This assertion appeared to be informed by his study of three LTT alloys for possible application in the welding of high-strength steel (Kromm et al., 2009). Table 6 shows the compositions of the three LWM: 7.33Ni, 9.44Ni and 10.81Ni respectively and the 2-pass welding used in their study. Essentially Ni was varied while other alloying elements were generally kept constant. Table 7

Fig. 20(a), (b) & (c) show the microstructures of the final and first passes of the three alloys. The microstructures showed that volume fraction of γ_r increased with increase in the Ni content – as indicated by the light etching. The first pass has been reheated by the final pass and the γ_r with its segregation has been refined. Fig. 20(d) & (e) show the final and middle pass microstructures of LTT alloy obtained in our ongoing study for 3-pass weld. The LTT microstructures varied along the weld beads. The mid pass that experienced reheating was refined and the γ_r uniformly dispersed (see Fig. 20(e)). This refinement may produce more ά in the mid-section and possibly the CRS that first formed at the weld surface due to rapid cooling could be reduced or even become tensile when the inner zone has completely transformed. It has even been reported that due to the inhomogeneous transformation in multi-pass weld or where the molten metal is large, the CRS at the weld surface can change to tensile after the transformation in the centre is completed (Nitschke-Pagel and Wohlfahrt, 2002). This would be due to delayed transformation of ά in the weld core, resulting to CRS in the inner zone and TRS at the surface. Fig. 21

The effect of microstructural refinement and uneven solute distribution on FCG in thick sections has not been reported. What has been studied well is the effect of the CRS on fatigue property of usually laboratory scales. (Saida et al., 2010) studied Cr/Ni WM containing Ni content in the range 7 – 10 wt% and 13Cr wt% (generally constant). They also reported that increase in the amount of Ni increased γ_r. The WM γ_r decreased TS (confirming Fig. 18), but it increased the impact energy at −30 °C test temperature. The cracking due to Ni segregation mentioned in Kromm's study was not reported. He also reported that WM containing 40–50% δ-ferrite minimized hot cracking susceptibility. (Kromm et al., 2011) suggested that designing LTT alloy with chemical compositions that will give dendritic solidification of WMs will reduce hot cracking. This view was supported by Saida, et al. and they also mentioned that γ_r can trap hydrogen thereby reducing cold cracking or hydrogen cracking in high strength steels.

Some factors affecting LTT weld alloys

It is important to note that most early studies on the LTT alloy were on small-thickness plates where just single- or two-pass weld filled the joint groove. For a single pass, the CRS induced by the LTT weld metal is unaltered, hence, effective in mitigating tensile stress in the weld. Multi LTT weld layers generated CRS, but the final state could be altered significantly (Z Feng et al., 2021) (Wang et al., 2018) (Novotný et al., 2016). In a multipass, the reheating of the previous beads re-distributes the RS and could convert the prior compressive state of the WM to tensile state (Nitschke-Pagel and Wohlfahrt, 2002). As already discussed, the performance of the LTT alloy in multipass weld thus depend on the T_i (Moat et al., 2018). Different T_i tends to create different RS fields. If the T_i is less than $Ms._T$, TRS zones could build up – eliminating or reducing the beneficial CRS (Moat et al., 2018) (Nitschke-Pagel and Wohlfahrt, 2002) (Thibault et al., 2010). To take advantage of the transformation plasticity in mitigating the RS, the T_i for the weld beads is expected to be above the $Ms._T$ so that γ matrix is maintained throughout. Thus, at the end of the weld runs, the whole of the WM transforms to ά upon cooling to T_a. In this case, the beneficial CRS is fully obtained (Moat et al., 2018) (Novotný et al., 2016). The use of low T_i would result to repeated ά formation in the previously deposited layer. Thus, taking T_i into account is an important factor in the usage of LTT alloys in multipass weld. The number of beads and the layering strategy affect LTT performance (Miki et al., 2012). Studies (Hensel et al., 2020) (Hensel et al., 2015) show that the performance of LTT can vary for

Table 7
Chemical composition of LWMs and joint geometry in (Kromm et al., 2009) study.

	Chemical composition of weld metal (wt.%)						
LTT alloy	C	Ni	Cr	Mn	Si	$Ms._T$ Cal	
7.33Ni	0.07	7.33	9.52	1.05	0.45	207	
9.44Ni	0.06	9.44	9.57	1.05	0.45	175	
10.81Ni	0.08	10.81	9.19	1.00	0.40	150	

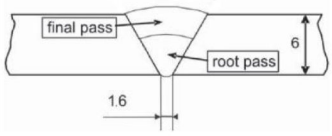

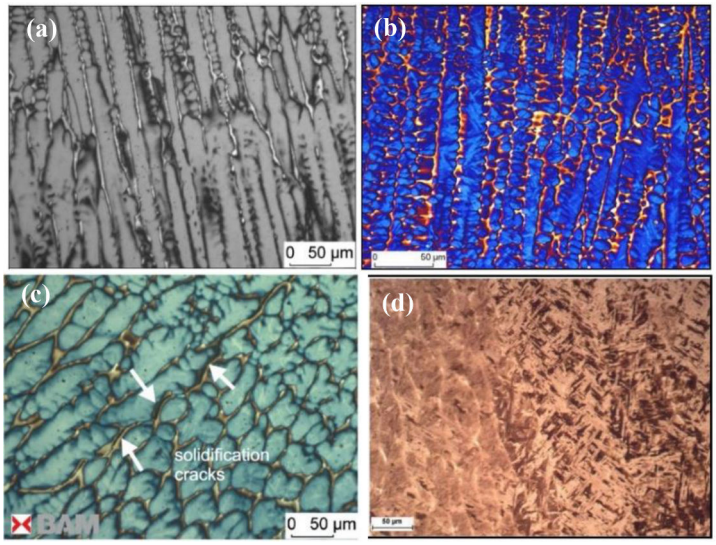

Fig. 20. Typical microstructures of LTT welding alloys (Kromm, 2014) (Kromm, 2011) (Kromm et al., 2011).

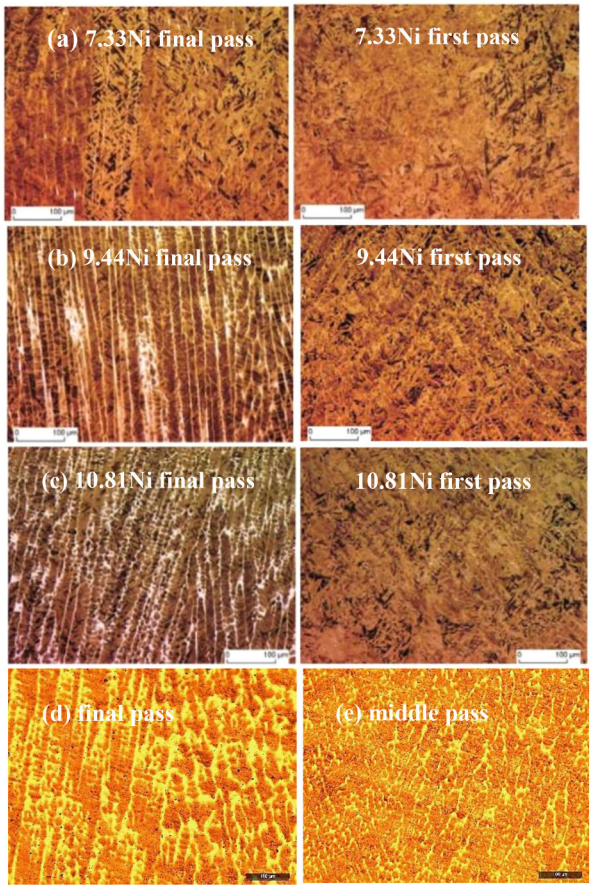

Fig. 21. Microstructures of LWMs (Kromm et al., 2009).

different steel grades. The type of joint also have strong influence on the LTT performance (Hensel et al., 2020). Weld geometry and dilution have been reported to affect the performance of LTT alloys (Karlsson, 2009) (Hosseini et al., 2020) (Sun et al., 2020) (Mikami et al., 2009). The dilution tends to increase or decrease the $Ms._T$ against the designed value. Compositional mismatch may lead to galvanic corrosion in some high strength steel in marine environment. These LTTWs induce CRS, however, excessive CRS at the weld toe could place the weld root in tension and then move the fatigue crack initiation point to the weld root (Eckerlid et al., 2003). The benefit and stability of the CRS induced by a particular LTT alloy can vary in different materials under the same loading conditions (Hensel et al., 2020). RS can vary for the same LTT alloy due to joint type and layering strategy (Miki et al., 2012). Increasing Cr and Ni elements result to high FS in the weld joint of high strength steels (Harati et al., 2017), but a maximum was obtained in the Ni increase beyond which the fatigue-enhancing CRS in the weld is decreased due to incomplete ά transformation at T_a (Hosseini et al., 2020).

Designing a LTT alloy is not a straightforward endeavour as many factors need to be considered. There is still no rigorously established trend on the benefit of LTT alloy in multipass welding that cuts across many conditions. To use LTT in multipass welding many factors need to be evaluated, ranging from steel grade, plate dimensions, type of loading, type of joint, heat source, type of LTT alloy, $Ms._T$, T_i, layering method, dilution effect and desired RS mitigation level in the weldment. We believe these are some of the issues that have been the bane of economic commercialization of LTT alloys. It appears that the best for now is to tailor all the conditions in the design of LTT alloy for welding a specific type of steel and dimension. There are also other issues of LTT alloy associated with the fatigue performance. The RS state of a body containing crack relaxes and redistribute as the crack grows (Hensel et al., 2015). The benefit of the LTT may be decreased or eliminated where the welded structure is subjected to overload capable of causing redistribution of stresses and plastic deformation (Eckerlid et al., 2003) (Karlsson, 2009) (Hensel et al., 2015). In other words, though LTT can induce CRS, but this effect can be relaxed under spectrum loading (Barsoum and Gustafsson, 2009). Thus, the stress waveform can affect the LTT fatigue performance. The YS of the γ is much lower than that of the ά (Bhadeshia et al., 2007) and will easily deform plastically. At high applied stresses, it can yield resulting to RS relaxation. Under cyclic loading, we saw that both TRS and CRS in the vicinity of the crack tip can redistribute (Miki et al., 2012) (Hensel et al., 2020) (Hensel et al., 2015). The γ is reported to have high work-hardening rates due to their low stacking fault energies (McGuire, 2008). Repeated plastic zone deformation can strain-harden the γ local to the crack tip. The γ_r can be metastable and with carbon composition greater than 0.02%, it can precipitate carbides. If the Ni composition is sufficient, ά can form under externally applied load (McGuire, 2008). In other words, in a situation where the γ_r contains considerable amount of alloying solutes at room temperature, strain-induced ά that enhances strengthening may occur under cyclic loading. Also, γ grain size refinement can increase the YS.

Thus, simultaneous hardening and softening under fatigue may occur in the crack tip vicinity when γ_r is present. This may explain the mode of stress relaxation and redistribution behaviour observed in fatigue behaviour of LTT alloys (Miki et al., 2012) (Hensel et al., 2020) (Hensel et al., 2015) (Z Feng et al., 2021). Increasing both strength and ductility is found to retard fatigue crack growth (FCG) (Igwemezie et al., 2019) (Igwemezie et al., 2018). Thus, structures under cyclic loading needs LTT filler that have high strength and good ductility and may not necessarily have low $Ms._T$ or high CRS at the weld toe or root. Though the high CRS retards fatigue crack initiation, but once the crack is nucleated the usefulness of LTT is drastically diminished. There are limited studies on the FCG behaviour of these alloys. FCGR comparative studies similar to Refs (Igwemezie et al., 2019) (Igwemezie et al., 2018) (Igwemezie and Mehmanparast, 2020) need to be carried out to increase the understanding and industrial usefulness of these welding alloys. This is because an LTT weld that seemingly have large CRS at weld toes may have large TRS in the mid-section of the weld. Immediately the crack traverses the compressive field, the internal TRS can assist in undesirable rapid crack propagation.

Conclusions and future work

The development, fatigue application and performance results of welding alloys to mitigate TRS, distortion and cracking in welded components have been reviewed in this paper. Tremendous work has been done to understand these LTT alloys by many researchers. Previous studies showed that LTT alloys can reduce the risk of fatigue failure and appears to be particularly useful for few weld passes and field repair where PWHT or peening is difficult or impractical. The LTT alloys performed better than the conventional fillers and FS was reported to be improved many times over without post-weld heat treatment. However, the benefit of LTTW in welding thick plates with multi beads would need to be carefully evaluated with respect to steel grade, plate thickness, joint type, number of weld passes, layering technique, heat source, dilution, fatigue loading under constant and variable frequencies, fatigue waveform and crack propagation effects on RS. It is found in the literature that these factors affect the performance of LTT alloys. The γ_r is also found to affect the effectiveness or the level of CRS induced by LWM. The effect of microstructural refinement or uneven solute distribution on fatigue crack initiation and growth in thick sections has not been reported. The role of microconstituents variations in the redistribution of the RS under cyclic loading is not available. Also, the FCG resistance performance data of these alloys under different frequencies and in marine conditions appears to be lacking. In thick steel plates, cracks are allowed to propagate to certain length before repair work is carried out. Future work demands that we understand how fatigue cracks grow in these LTT alloys and its associated heat affected zone under multipass conditions.

Funding

The funding through EPSRC – Doctoral prize is acknowledged.

Declaration of Competing Interest

The authors declare that they have no known competing financial interests or personal relationships that could have appeared to influence the work reported in this paper.

References

Abdullah, A., Malaki, M., Eskandari, A., 2012. Strength enhancement of the welded structures by ultrasonic peening. Mater. Des. 38, 7–18. https://doi.org/10.1016/j.matdes.2012.01.040.

Ainsworth, R.A., Sharples, J.K., Smith, S.D., 2000. Effects of residual stresses on fracture behaviour - experimental results and assessment methods. J. Strain Anal. Eng. Des. 35, 307–316. https://doi.org/10.1243/0309324001514431.

Alghamdi, T., Liu, S., 2014. Low Transformation Temperature (LTT) Welding Consumables for Residual Stress Management : consumables Development and Testing Qualification. Weld. J. 93, 243–251.

Barsoum, Z., Gustafsson, M., 2009. Fatigue of high strength steel joints welded with low temperature transformation consumables. Eng. Fail. Anal. 16, 2186–2194. https://doi.org/10.1016/j.engfailanal.2009.02.013.

Bhadeshia, H., Honeycombe, R., 2006. Steels: Microstructure and Properties. Steels Microstruct Prop.

Bhadeshia H.K.D.H., Francis J.A., Stone H.J., Kundu S., Rogge R.B., Withers P.J., et al. Transforamtion Plasticity in Steel Weld Metals. Proceeding 10th Int Aachen Weld Conf 2007.

Bhadeshia, H.K.D.H., 2002a. Handbook of Residual Stress and Deformation of Steel. ASM International.

Bhadeshia, H.K.D.H., 2002b. TRIP-Assisted Steels? ISIJ Int. 42, 1059–1060.

Bhadeshia, H.K.D.H., 2004. Developments in martensitic and bainitic steels: role of the shape deformation. Mater. Sci. Eng. A 378, 34–39.

Bhatti, A.A., Barsoum, Z., Van Der Mee, V., Kromm, A., Kannengiesser, T., 2013. Fatigue strength improvement of welded structures using new low transformation temperature filler materials. Procedia Eng. 66, 192–201. https://doi.org/10.1016/j.proeng.2013.12.074.

Bolton, J.D., Petty, E.R., Allen, G.B., 1971. The mechanical properties of α-phase low-carbon Fe-Mn alloys. Metall. Trans. 2, 2915–2923.

Capdevila, C., Caballero, F.G., García De Andrés, C., 2002. Determination of Ms temperature in steels: a Bayesian neural network model. ISIJ Int. 42, 894–902. https://doi.org/10.2355/isijinternational.42.894.

Cheng, X., Fisher, J.W., Prask, H.J., Gnäupel-Herold, T., Yen, B.T., Roy, S., 2003. Residual stress modification by post-weld treatment and its beneficial effect on fatigue strength of welded structures. Int. J. Fatigue 25, 1259–1269. https://doi.org/10.1016/j.ijfatigue.2003.08.020.

Choi, S., Lee, J., Lee, J.Y., Kang, S.K., Kim, Y.C., Lee, S.J., et al., 2021. Effect of low transformation temperature welding consumable on microstructure, mechanical properties and residual stress in welded joint of A516 carbon steel. J. Korean Inst. Met. Mater. 59, 524–532. https://doi.org/10.3365/KJMM.2021.59.8.524.

Colegrove, P., Ikeagu, C., Thistlethwaite, A., Williams, S., Nagy, T., Suder, W., et al., 2009. The welding process impact on residual stress and distortion. Sci. Technol. Weld. Join. 14, 717–725.

Coules, H.E., 2013. Contemporary approaches to reducing weld induced residual stress. Mater. Sci. Technol. (United Kingdom) 29, 4–18. https://doi.org/10.1179/1743284712Y.0000000106.

Deng, D., Murakawa, H., 2013. Influence of transformation induced plasticity on simulated results of welding residual stress in low temperature transformation steel. Comput. Mater. Sci. 78, 55–62. https://doi.org/10.1016/j.commatsci.2013.05.023.

De Souza, L.F.G., De Souza Bott, I., Jorge, J.C.F., Guimaraes, A.S., Paranhos, R.P.R, 2005. Microstructural analysis of a single pass 2.25% Cr–1.0% Mo steel weld metal with different manganese contents. Mater. Charact. 55, 19–27.

Eckerlid, J., Nilsson, T., Karlsson, L., 2003. Fatigue properties of longitudinal attachments welded using low transformation temperature filler. Sci. Technol. Weld. Join 8, 353–359. https://doi.org/10.1179/136217103225005525.

Feng, Z., Ma, N., Tsutsumi, S., Di, X., 2021a. Size effect on residual stress in low transformation temperature welded joints. Mar. struct. 78, 103001 https://doi.org/10.1016/j.marstruc.2021.103001.

Feng, Z., Ma, N., Tsutsumi, S., Lu, F., 2021b. Investigation of the residual stress in a multi-pass t-welded joint using low transformation temperature welding wire. Materials (Basel) 14, 1–15. https://doi.org/10.3390/ma14020325.

Francis, J.A., Bhadeshia, H.K.D.H., Withers, P.J., 2007a. Welding residual stresses in ferritic power plant steels. Mater. Sci. Technol. 23, 1009–1020. https://doi.org/10.1179/174328407X213116.

Francis, J.A., Kundu, S., Bhadeshia, H.K.D.H., Stone, H.J., Rogge, R.B., Withers, P.J., et al., 2007b. Transformation Temperatures and Welding Residual Stresses in Ferritic Steels. Proc. PVP2007 2007. ASME Press. Vessel. Pip. Div. Conf., pp. 949–956

Fricke, W., 2005. Effects of residual stresses on the fatigue behaviour of welded steel structures. Mater. Sci. Eng. Technol. 36, 642–649. https://doi.org/10.1002/MAWE.200500933.

Grong, O., Matlock, D.K., 2013. Microstructural development in mild and low-alloy steel weld metals. Int. Met. Rev. 31, 27–48. https://doi.org/10.1179/IMTR.1986.31.1.27.

Habibi, N., H-Gangaraj, S.M., Farrahi, G.H., Majzoobi, G.H., Mahmoudi, A.H., Daghigh, M., et al., 2012. The effect of shot peening on fatigue life of welded tubular joint in offshore structure. Mater. Des. 36, 250–257. https://doi.org/10.1016/j.matdes.2011.11.024.

Harati, E., Karlsson, L., Svensson, L.E., Dalaei, K., 2017. Applicability of low transformation temperature welding consumables to increase fatigue strength of welded high strength steels. Int. J. Fatigue 97, 39–47. https://doi.org/10.1016/j.ijfatigue.2016.12.007.

Heinze C., Pittner A., Rethmeier M., Babu S.S. Dependency of Martensite Start Temperature On Prior Austenite Grain Size and Its Influence On Welding-Induced Residual Stresses 2013. 10.1016/j.commatsci.2012.11.058.

Hensel, J., Nitschke-Pagel, T., Dixneit, J., Dilger, K., 2020. Capability of martensitic low transformation temperature welding consumables for increasing the fatigue strength of high strength steel joints. Mater. Test. 62, 891–899. https://doi.org/10.3139/120.111562.

Hensel, J., Nitschke-Pagel, T., Rebelo-Kornmeier, J., Dilger, K., 2015. Experimental Investigation of Fatigue Crack Propagation in Residual Stress Fields. Procedia Eng. 133, 244–254. https://doi.org/10.1016/j.proeng.2015.12.664.

Hosseini, S.A., Gheisari, K., Moshayedi, H., Ahmadi, M.R., Warchomicka, F., Enzinger, N., 2021. Assessment of the chemical composition of LTT fillers on residual

stresses, microstructure, and mechanical properties of 410 AISI welded joints. Weld World 65, 807–823. https://doi.org/10.1007/s40194-020-01064-1.
Hosseini, S.A., Gheisari, K., Moshayedi, H., Warchomicka, F., Enzinger, N., 2020. Basic alloy development of low-transformation-temperature fillers for AISI 410 martensitic stainless steel. Sci. Technol. Weld Join 25, 243–250. https://doi.org/10.1080/13621718.2019.1681159.
Igwemezie, V., Dirisu, P., Mehmanparast, A., 2019. Critical assessment of the fatigue crack growth rate sensitivity to material microstructure in ferrite-pearlite steels in air and marine environment. Mater. Sci. Eng. A 754. https://doi.org/10.1016/j.msea.2019.03.093.
Igwemezie, V., Mehmanparast, A., Kolios, A., 2018. Materials selection for XL wind turbine support structures: a corrosion-fatigue perspective. Mar. struct. 61, 381–397. https://doi.org/10.1016/J.MARSTRUC.2018.06.008.
Igwemezie, V., Mehmanparast, A., 2020. Waveform and frequency effects on corrosion-fatigue crack growth behaviour in modern marine steels. Int. J. Fatigue 134. https://doi.org/10.1016/j.ijfatigue.2020.105484.
Igwemezie V.C., Ugwuegbu C.C., Mark U. Physical Metallurgy of Modern Creep-Resistant Steel for Steam Power Plants: microstructure and Phase Transformations. J Metall 2016:1–19. 10.1155/2016/5468292.
Izumiyama, M., Tsuchiya, M., Imai, Y., 1970. Effects of alloying element on supercooled A3 transformation of iron. Sci. Rep. Res. Institutes Iron, Steel Other Met Tohoku Univ 22, 105–115.
Jiang, W., Chen, W., Woo, W., Tu, S.-T., Zhang, X.-C., Em, V, 2018. Effects of low-temperature transformation and transformation-induced plasticity on weld residual stresses: numerical study and neutron diffraction measurement. Mater. Des. 147, 65–79.
Jones, W.K.C., Alberry, P.J., 1977. A model for stress accumulation in steels during welding. Met. Technol. 11, 557–566.
Karlsson, L., Mraz, L., 2011. Increasing fatigue life using Low Transformation Temperature (LTT) welding consumables. Zváranie Svarováni 1–2, 8–15.
Karlsson, L., 2009. Improving fatigue life with Low Temperature Transformation (LTT) welding consumables. in SVETSAREN 64.
Kou, S., 2003. Welding Metallurgy, 2nd ed. John Wiley & Sons, Inc., New Jersey.
Kromm, A., Kannengiesser, T., Altenkirch, J., Gibmeier, J., 2011. Residual Stresses in Multilayer Welds with Different Martensitic Transformation Temperatures Analyzed by High-Energy Synchrotron Diffraction. Mater. Sci. Forum 681, 37–42. https://doi.org/10.4028/www.scientific.net/MSF.681.37.
Kromm, A., Kannengiesser, T., Gibmeier, J., Genzel, C., van der, Mee V, 2009. Determination of residual stresses in low transformation temperature (LTT-) weld metals using X-ray and high energy synchrotron radiation. Weld World 53, 3–16.
Kromm, A., 2011. Transformation Behavior and Residual Stresses When Welding New Types of LTT Filler Materials. Otto von Guericke University Magdeburg.
Kromm, A., 2014. Residual stress engineering by low transformation temperature alloys - state of the art and recent developments. Weld World 58, 729–741.
Leggatt, R.H., 2008. Residual stresses in welded structures. Int. J. Press Vessel Pip. 85, 144–151. https://doi.org/10.1016/j.ijpvp.2007.10.004.
Li, Y., San Martín, D., Wang, J., Wang, C., Xu, W., 2021. A review of the thermal stability of metastable austenite in steels: martensite formation. J. Mater. Sci. Technol. 91, 200–214. https://doi.org/10.1016/j.jmst.2021.03.020.
Masubuchi, K., 1980a. Analysis of Welded structures : Residual stresses, distortion, and Their Consequences, 1st ed., 33. Pergamon Press, Oxford; New York.
Masubuchi, K., 1980b. Analysis and Control of Residual Stresses, Distortion and Their Consequences in Welded Structures, 33. Pergamon Press, Oxford; New York.
McGuire M. Stainless Steels for Design Engineers. Materials Park, OH 44073-0002: ASM International; 2008. 10.1361/ssde2008p001.
Mikami, Y., Morikage, Y., Mochizuki, M., Toyoda, M., 2009. Angular distortion of fillet welded T joint using low transformation temperature welding wire. Sci. Technol. Weld. Join 14, 97–105. https://doi.org/10.1179/136217108X382972.
Miki, C., Hanji, T., Tokunaga, K., 2012. Weld repair for fatigue-cracked joints in steel bridges by applying low temperature transformation welding wire. Weld. World 56, 40–50. https://doi.org/10.1007/BF03321334.
Miyata, M., Suzuki, R., 2015. Welding process and consumables aimed at improving fatigue strength of joints. R D Res. Dev. Kobe Steel Eng. Rep. 65, 16–20.
Moat, R.J., Ooi, S., Shirzadi, A.A., Dai, H., Mark, A.F., Bhadeshia, H.K.D.H., et al., 2018. Residual stress control of multipass welds using low transformation temperature fillers. Mater. Sci. Technol. (United Kingdom) 34, 519–528. https://doi.org/10.1080/02670836.2017.1410954.
Moat, R.J., Stone, H.J., Shirzadi, A.A., Francis, J.A., Kundu, S., Mark, A.F., et al., 2011. Design of weld fillers for mitigation of residual stresses in ferritic and austenitic steel welds. Sci. Technol. Weld. Join 16, 279–284. https://doi.org/10.1179/1362171811Y.0000000003.
Nitschke-Pagel, T., Wohlfahrt, H., 2002. Residual stresses in welded joints - Sources and consequences. Mater. Sci. Forum 404–407, 215–226. https://doi.org/10.4028/www.scientific.net/msf.404-407.215.
Nose T., Okawa T. Approaches for fundamental principles 2: total solution for fatigue of steel. 2012.
Novotný, L., de Abreu, H.F.G., de Miranda, H.C., Béreš, M., 2016. Simulations in multipass welds using low transformation temperature filler material. Sci. Technol. Weld. Join 21, 680–687. https://doi.org/10.1080/13621718.2016.1177989.
Ohta, A., Matsuoka, K., Nguyen, N.T., Maeda, Y., Suzuki, N., 2003. Fatigue strength improvement of lap joints of thin steel plate using low-transformation-temperature welding wire. Weld J. (Miami, Fla) 82.
Ohta, A., Suzuki, N., Maeda, Y., Hiraoka, K., Nakamura, T., 1999a. Superior fatigue crack growth properties in newly developed weld metal. Int. J. Fatigue 21, 113–118. https://doi.org/10.1016/s0142-1123(99)00062-6.
Ohta, A., Suzuki, N., Maeda, Y., Hiraoka, K., Nakamura, T., 1999b. Superior fatigue crack growth properties in newly developed weld metal 21.
Ohta A., Watanabe O., Matsuoka K., Maeda Y., Suzuki N., Kubo T. Fatigue strength improvement of box welds by low transformation temperature welding wire by PWHT. Int. Inst. Weld. 1999;Document X.
Ooi, S.W., Garnham, J.E., Ramjaun, T.I., 2014. Review: low transformation temperature weld filler for tensile residual stress reduction. Mater. Des. 56, 773–781. https://doi.org/10.1016/j.matdes.2013.11.050.
Orr S. Impeller Fatigue Assessment Using an S-N Approach. AMCA Int. Eng. Conf., Las Vegas, NV, USA: 2008.
Ota, A., Maeda, Y., Suzuki, N., Watanabe, O., Kubo, T., Katsuoka, K., 2001. Fatigue strength improvement of box welds using low transformation temperature welding material. Tripled fatigue strength by post weld heat treatment. Weld. Int. 19, 373–376. https://doi.org/10.1080/09507110209549487.
Ota, A., Shiga, C., Maeda, Y., Suzuki, N., Watanabe, O., Kubo, T., et al., 2000. Fatigue strength improvement of box-welded joints using low transformation temperature welding material. Weld. Int. 14, 801–805. https://doi.org/10.1080/09507110009549271.
Peet, M., 2014. Prediction of martensite start temperature. Mater. Sci. Technol. 31, 1370–1375.
Saida, K., Nishimoto, K., Ogawa, K., Okaguchi, S., Fujiwara, K., 2010. Proposal of welding consumable of triplex stainless steel for ultrahigh strength steel. Sci. Technol. Weld. Join 15, 185–193. https://doi.org/10.1179/136217109X12568132624406.
Satoh, K., Matsui, S., Machida, T., 1966. Thermal Stresses Developed In High-strength Steels Subjected To Thermal Cycles Simulating Weld Heat-affected Zone. J. Japan Weld. Soc. 35, 780–789. https://doi.org/10.2207/qjjws1943.35.9_780.
Satoh, K., 1966. Thermal stress generation process and residual stress in high-strength steel welds. J. Japan Weld. Soc. 35, 780–789.
Shiga, C., Yasuda, H.Y., Hiraoka, K., Suzuki, H., 2010. Effect of Ms temperature on residual stress in welded joints of hig- strength steels. Weld World 54.
Shirzadi, A.A., Bhadeshia, H.K.D.H., Karlsson, L., Withers, P.J., 2009. Stainless steel weld metal designed to mitigate residual stresses. Sci. Technol. Weld. Join 14, 559–565. https://doi.org/10.1179/136217109X437178.
Shirzadi, A.A., 2019. Modelling and design of new stainless-steel welding alloys suitable for low-deformation repairs and restoration processes. Procedia Manuf. 37, 627–632. https://doi.org/10.1016/j.promfg.2019.12.099.
Sun, Y.L., Hamelin, C.J., Vasileiou, A.N., Xiong, Q., Flint, T.F., Obasi, G., et al., 2020. Effects of dilution on the hardness and residual stresses in multipass steel weldments. Int. J. Press Vessel Pip. 187, 104154 https://doi.org/10.1016/j.ijpvp.2020.104154.
Suzuki, N., Ohta, A., Maeda, Y., 2004. Repair of fatigue cracks initiated around box welds using low transformation temperature welding material. Weld. Int. 18, 112–117. https://doi.org/10.1533/wint.2004.3221.
Thibault, D., Bocher, P., Thomas, M., Gharghouri, M., Côté, M., 2010. Residual stress characterization in low transformation temperature 13%Cr-4%Ni stainless steel weld by neutron diffraction and the contour method. Mater. Sci. Eng. A 527, 6205–6210. https://doi.org/10.1016/j.msea.2010.06.035.
Thomas, S.H., Liu, S., 2014. Analysis of low transformation temperature welding (LTTW) consumables - Distortion control and evolution of stresses. Sci. Technol. Weld. Join 19, 392–401. https://doi.org/10.1179/1362171814Y.0000000199.
Thomson, R.C., 1992. Carbide Composition Changes in Power Plant Steels as a Method of Remanent Creep Life Prediction. University of Cambridge.
Wang, H., Woo, W., Kim, D.K., Em, V., Lee, S.Y, 2018. Effect of chemical dilution and the number of weld layers on residual stresses in a multi-pass low-transformation-temperature weld. Mater. Des. 160, 384–394. https://doi.org/10.1016/j.matdes.2018.09.016.
Wang, W.X., Huo, L.X., Zhang, Y.F., Wang, D.P., Jing, H.Y., 2002. New developed welding electrode for improving the fatigue strength of welded joints. J. Mater. Res. Technol. Mater. Sci. Technol. 18, 527–531.
Watanabe, O., Matsumoto, S., Nakano, Y., Saito, Y., 1995. Fatigue strength of welded joint of high strength steel and its controlling factor. Effects of stress concentration factor and welding residual stress. Yosetsu Gakkai Ronbunshu (Quarterly J Japan Weld Soc 13, 438–443.
Withers, P.J., Bhadeshia, H.K.D.H., 2001a. Residual stress part 2 - Nature and origins. Mater. Sci. Technol. 17, 366–375. https://doi.org/10.1179/026708301101510087.
Withers, P.J., Bhadeshia, H.K.D.H., 2001b. Residual stress part 1 - Measurement techniques. Mater. Sci. Technol. 17, 355–365. https://doi.org/10.1179/026708301101509980.
Wu, S., Wang, D., Di, X., Zhang, Z., Feng, Z., Liu, X., et al., 2018. Toughening mechanisms of low transformation temperature deposited metals with martensite–austenite dual phases. J. Mater. Sci. 53, 3720–3734. https://doi.org/10.1007/s10853-017-1766-2.
Wu, S., Wang, D., Zhang, Z., Li, C., Liu, X., Zhou, Z., et al., 2019. Effect of dilution on fatigue behaviour of welded joints produced by low-transformation-temperature fillers. Sci. Technol. Weld. Join 24, 601–608. https://doi.org/10.1080/13621718.2019.1576272.
Wu, X., Wang, Z., Yu, Z., Liu, S., Bunn, J.R., Kolbus, L., et al., 2020. Control of Weld Residual Stress in a Thin Steel Plate through Low Transformation Temperature Welding Consumables. Weld J 99, 124s–134s. https://doi.org/10.29391/2020.99.012.
Yang, H.-S., Bhadeshia, H.K.D.H., 2009. Austenite grain size and the martensite-start temperature. Scr. Mater. 60, 493–495. https://doi.org/10.1016/j.scriptamat.2008.11.043.
Yang, H.S., Woo Suh, D., Kumar, H., Bhadeshia, D.H, 2012. More Complete Theory for the Calculation of the Martensite-Start Temperature in Steels. ISIJ Int. 52, 164–166.

Zenitani, S., Hayakawa, N., Yamamoto, J., Hiraoka, K., Morikage, Y., Kubo, T., et al., 2007. Development of new low transformation temperature welding consumable to prevent cold cracking in high strength steel welds. Sci. Technol. Weld. Join 12, 516–522. https://doi.org/10.1179/174329307X213675.

Zerbst, U., 2020. Application of fracture mechanics to welds with crack origin at the weld toe—A review. Part 2: welding residual stresses. Residual and total life assessment. Weld. World 64, 151–169. https://doi.org/10.1007/s40194-019-00816-y.

Zhang, Z., Farrar, R.A., 1995. Columnar grain development in C-Mn-Ni low-alloy weld metals and the influence of nickel. J. Mater. Sci. 30, 5581–5588.

2022-04-06

A review of LTT welding alloys for structural steels: design, application and results

Igwemezie, Victor C.

Elsevier

Igwemezie V, Shamir M, Mehmanparast A, Ganguly S. (2022) A review of LTT welding alloys for structural steels: design, application and results. Journal of Advanced Joining Processes, Volume 5, June 2022, Article number 100110

https://doi.org/10.1016/j.jajp.2022.100110